Calculation of displacement correlation tensor indicating vortical cooperative motion in two-dimensional colloidal liquids

Ooshida Takeshi (大信田 丈志)*
Department of Mechanical and Aerospace Engineering, Tottori University, Tottori 680-8552, Japan

Susumu Goto (後藤 晋)
Graduate School of Engineering Science, Osaka University, Toyonaka, Osaka 560-8531, Japan

Takeshi Matsumoto (松本 剛)
Division of Physics and Astronomy, Graduate School of Science, Kyoto University, Kyoto 606-8502, Japan

Michio Otsuki (大槻 道夫)
Department of Materials Science, Shimane University, Matsue 690-8504, Japan
(Received 12 April 2016; revised manuscript received 22 July 2016; published 18 August 2016)

As an indicator of cooperative motion in a system of Brownian particles that models two-dimensional colloidal liquids, a displacement correlation tensor is calculated analytically and compared with numerical results. The key idea for the analytical calculation is to relate the displacement correlation tensor, which is a kind of four-point space-time correlation, to the Lagrangian two-time correlation of the deformation gradient tensor. Tensorial treatment of the statistical quantities, including the displacement correlation itself, allows capturing the vortical structure of the cooperative motion. The calculated displacement correlation also implies a negative long-time tail in the velocity autocorrelation, which is a manifestation of the cage effect. Both the longitudinal and transverse components of the displacement correlation are found to be expressible in terms of a similarity variable, suggesting that the cages are nested to form a self-similar structure in the space-time.

DOI: 10.1103/PhysRevE.94.022125

I. INTRODUCTION

Cooperative motions of densely packed particles [1,2] are now generally recognized as an essential ingredient of the statistical mechanics of such a system, and their characterization and quantification make up one of the central problems in the area [3,4]. These cooperative motions are often found to consist of swirls or vortices [5–8], reminiscent of the vortices of momentum observed in other systems [9,10]. Similar vortex patterns are now known to appear frequently in systems of self-propelled units (both living and nonliving) [11]. Having observed these conspicuous vortices in systems of molecular, colloidal, granular, and self-propelled particles, we raise the following questions: Can we incorporate such vortices into the statistical theory of the particles, so as to understand certain aspects of their dynamics *quantitatively*? In particular, is it possible to calculate statistical quantities indicating vortical cooperative motion in systems in which momentum is *not* conserved, such as colloidal liquids subject to Langevin dynamics?

The question of quantitative theory with vortices is quite challenging, as is seen in analogous attempts in the research of fluid turbulence that is filled with vortex tubes, blobs, and sheets [12]. The velocity fluctuations of high Reynolds-number turbulence are characterized by statistical scaling laws [12–15], which are not yet understood on the basis of the first principles, namely, by solving the Navier-Stokes equation. As an approach based on vortical solutions to the Navier-Stokes equation, we may mention theoretical calculation of velocity statistics from superposition of a specific vortical pattern [16]. It is criticizable, however, that the choice of the vortex model and the assumption on the distribution of the vortex patterns are rather arbitrary, as was pointed out by the authors themselves [17].

In the background of the second question, motivated by the suspect that momentum conservation is not essential to the vortical cooperative motion, there is a fact that different space-time correlations have been devised for different systems. While the equal-time correlation of velocity is already informative in some systems, a more elaborate statistical quantity is often needed for other systems. In the case of colloidal suspensions as model glassy systems, the most widely used idea is to focus on the density field, $\rho(\mathbf{r},t)$, and define its four-point space-time correlation by analogy with spin glasses [3,18,19]. In this context, the case of dense liquids subject to Newtonian molecular dynamics deserves special consideration. Indeed, momentum is conserved in such systems, but their long-time behavior is known to be basically the same as that of colloidal glasses [20–22]. The cooperative motions in dense molecular liquids seem rather to stem from mass conservation, and a popular approach to this cooperativity is, again, based on four-point space-time correlations of $\rho(\mathbf{r},t)$.

A disadvantage of this approach is that, since $\rho(\mathbf{r},t)$ is scalar, it lacks direct access to the directional aspect of the cooperative motion. Admittedly, some refined scalar descriptions such as the many-particle density approach [23] are possible, but they are difficult to illustrate pictorially and therefore not very intuitive.

*ooshida@damp.tottori-u.ac.jp

Another approach to the cooperative motion is based on the displacement of the particles. Let us denote the displacement of the ith particle for the time interval from s to t with

$$\mathbf{R}_i = \mathbf{R}_i(t,s) = \mathbf{r}_i(t) - \mathbf{r}_i(s), \tag{1.1}$$

where $\mathbf{r}_i$ is the position vector of the particle. Indeed, $\mathbf{R}_i$ includes information of the direction of motion, but again this information was discarded in most of the existing studies, in which statistics of scalar quantities such as $\langle \mathbf{R}_i \cdot \mathbf{R}_j \rangle$ [1,24] or $\langle |\mathbf{R}_i||\mathbf{R}_j| \rangle$ [25] were computed.

The directionality, however, is crucial for understanding the cooperative motion, which often consists of vortices [6–8] as we have already noticed. Conversely, the space-time structure of the vortical motion is expected to contain information of the directional statistics of $\mathbf{R}_i$. In the context of glassy liquids, recently there appeared several studies on such statistics in connection with solid-like elasticity [26–29]. Now let us focus on a more pictorial illustration of directional statistics given by Doliwa and Heuer [5]: in their Fig. 8, the particles "in front" and "in back" of the central one, i.e., the particles with the relative position vector parallel to $\mathbf{R}_i$, have a very long-ranged directional correlation, while the "sideways" particles form a kind of backflow structure with a pair of swirls (as we will see later in Fig. 1). In other words, with $\mathbf{r}_{ij} = \mathbf{r}_j - \mathbf{r}_i$ denoting the relative position vector, the displacement correlation for $\mathbf{r}_{ij}$ parallel to $\mathbf{R}_i$ is considerably different from that for $\mathbf{r}_{ij}$ perpendicular to $\mathbf{R}_i$.

Mathematically, there is a simple way to retain the directional information in $\mathbf{R}_i$: instead of the inner product in $\langle \mathbf{R}_i \cdot \mathbf{R}_j \rangle$ in the preceding studies [1,24], we may adopt the tensorial product and study the *displacement correlation tensor* [30,31], which we denote symbolically with $\langle \mathbf{R}_i \otimes \mathbf{R}_j \rangle$ or $\langle \mathbf{R} \otimes \mathbf{R} \rangle$ (a more precise definition will be given later). The displacement correlation tensor, on one hand, includes essentially the same information as the parallel and perpendicular correlations defined by Doliwa and Heuer [5]. On the other hand, as the definition of $\langle \mathbf{R} \otimes \mathbf{R} \rangle$ is free from conditional angular summation used by Doliwa and Heuer [5], it is more amenable to analytical calculation [31].

In the present paper, we compare the analytical calculation of $\langle \mathbf{R} \otimes \mathbf{R} \rangle$ [31] with the numerical solutions of the Langevin dynamics as a model of two-dimensional (2D) colloidal liquids. The paper is organized as follows: In Sec. II the governing equation is specified together with simulation details. A continuum version of the governing equation is also given and some statistical quantities are defined, which forms a basis for the analytical calculation. Subsequently, in Sec. III the displacement correlation tensor is defined and computed numerically. Analytical calculation is then explained in Sec. IV, which is based on a rather crude approximation and intended as a springboard for a more elaborate theory in the future. Comparison between the numerical and analytical results is made in Sec. V; considering the limitations of the approximation, we find the two results to agree to a surprising extent, except for the short-range behavior. Possible relevance to glassy dynamics and future directions are discussed in Sec. VI, and finally, Sec. VII is allotted for concluding remarks.

II. SETUP

A. Specification of the particle system

We consider a system consisting of N Brownian particles in an n_d-dimensional periodic box of the size L^{n_d}, focusing on the 2D case and also paying some attention to the one-dimensional (1D) case, so that $n_\mathrm{d} = 2$ or $n_\mathrm{d} = 1$. The system is statistically steady and homogeneous, with the mean density $\rho_0 = N/L^{n_\mathrm{d}}$, being in equilibrium at the temperature T. The position vectors of the particles, denoted by $\mathbf{r}_i$ with $i = 1,2,\ldots,N$, are governed by the overdamped Langevin equation

$$\mu \dot{\mathbf{r}}_i = -\frac{\partial}{\partial \mathbf{r}_i} \sum_{j<k} V_{jk} + \mu \mathbf{f}_i(t), \tag{2.1}$$

where μ is the drag coefficient, and V_{jk} is the interaction potential between the jth and kth particles. The random forcing is Gaussian with the variance

$$\langle \mathbf{f}_i(t) \otimes \mathbf{f}_j(t') \rangle = 2D\delta_{ij}\delta(t-t')\mathbb{1}, \tag{2.2}$$

where $D = k_\mathrm{B}T/\mu$. The pair potential V_{jk} is repulsive and short-ranged, so that the particle diameter can be defined through the excluded volume effect. For concreteness, as a function of $r_{jk} = |\mathbf{r}_k - \mathbf{r}_j|$, we specify the potential as [28,32,33]

$$V_{jk} = \begin{cases} V_\mathrm{max}\left(1 - \dfrac{|r_{jk}|}{\sigma}\right)^2 & (|r_{jk}| \leqslant \sigma) \\ 0 & (|r_{jk}| > \sigma) \end{cases} \tag{2.3}$$

with σ denoting the diameter of the particles. To make V_{jk} close to the hardcore potential, sufficiently large values of V_max were used: the value is specified as $V_\mathrm{max}/k_\mathrm{B}T = 50$, unless noted otherwise.

Aside from the density $\rho_0 = N/L^2$ for $n_\mathrm{d} = 2$, we denote the area fraction with $\phi = (\pi/4)\sigma^2 N/L^2 = (\pi/4)\sigma^2\rho_0$. Numerical calculations are performed with $\phi = 0.50$ and $N = 4000$, unless specified otherwise. The initial condition is prepared by starting from a random configuration and equilibrating the system under the Langevin dynamics with the target temperature T, for sufficiently long waiting time (typically $20\,\sigma^2/D$). The computed results are nondimensionalized so that σ, D, and μ become equal to unity.

B. Continuum description

For the theoretical approach in Sec. IV, the overdamped Langevin equation for $\mathbf{r}_i(t)$ is rewritten in terms of the density field,

$$\rho = \rho(\mathbf{r},t) = \sum_j \rho_j(\mathbf{r},t), \tag{2.4}$$

where $\rho_j(\mathbf{r},t) = \delta^{n_\mathrm{d}}(\mathbf{r} - \mathbf{r}_j(t))$ at the finer level of description as the operator acting on $\mathbf{r}_j(t)$ [34], with $\delta^{n_\mathrm{d}}(\cdot)$ denoting the n_d-dimensional delta function, but in practice $\rho_j(\mathbf{r},t)$ should be regarded as its average over the local equilibrium ensemble [35,36]. The equation for ρ is customarily referred to as the Dean-Kawasaki equation [37–41]; it is a kind of stochastic diffusion equation [42–44], analogous to nonlinear stochastic equations describing mesoscopic kinetics of phase separation [45–47], though the appellation "Dean-Kawasaki" is limited to the one with a specific form of nonlinearity

prescribed below. It is convenient to express it as a set of two equations, consisting of the continuity equation,

$$\partial_t \rho + \nabla \cdot \mathbf{Q} = 0, \tag{2.5}$$

and a stochastic equation for the flux,

$$\mathbf{Q} = -D\left(\nabla\rho + \frac{\rho}{k_{\mathrm{B}}T}\nabla U\right) + \sum_j \rho_j(\mathbf{r},t)\mathbf{f}_j(t), \tag{2.6}$$

where $\mathbf{f}_j(t)$ denotes the random forcing subject to Eq. (2.2) and

$$U = U[\rho](\mathbf{r}) = \int V_{\mathrm{eff}}(r_*)\rho(\tilde{\mathbf{r}})\, d^2\tilde{\mathbf{r}} \quad (\text{for } n_{\mathrm{d}} = 2) \tag{2.7}$$

describes the interaction of the particles, with V_{eff} denoting the effective potential based on the direct correlation function [40,48,49], related to the static structure factor $S(k)$ explained below [in Eq. (2.8)], and $r_* = |\mathbf{r} - \tilde{\mathbf{r}}|$. Note that V_{eff} appears as a result of the coarse graining [35,36].

Elimination of $\mathbf{Q}$ from Eqs. (2.5) and (2.6) yields a single equation for $\rho(\mathbf{r},t)$ which is often taken as a starting point for nonlinear theory of glassy dynamics [41,50–53]. In Sec. IV, however, we will prefer to start from Eq. (2.6) without this elimination, in the hope that the presence of $\mathbf{Q}$ will be helpful in capturing the directional aspect of the cooperative motion. We emphasize that $\mathbf{Q}$ enters the theory not because it is momentum which may or may not be conserved, but because it is the flux of the conserved quantity ρ.

The static structure factor is defined by

$$S(k) = \frac{1}{N}\sum_{i,j}\langle e^{\mathrm{i}\mathbf{k}\cdot(\mathbf{r}_j - \mathbf{r}_i)}\rangle \quad (\mathbf{k} \neq \mathbf{0}) \tag{2.8}$$

based on a snapshot of the particle configuration. Evidently $S(k)$ equals the initial value of the intermediate scattering function (the dynamical structure factor):

$$F(k,t) = \frac{1}{N}\sum_{i,j}\langle e^{\mathrm{i}\mathbf{k}\cdot[\mathbf{r}_j(t) - \mathbf{r}_i(0)]}\rangle \quad (\mathbf{k} \neq \mathbf{0}). \tag{2.9}$$

For colloidal systems modeled by Eq. (2.1) with constant scalar μ (i.e., without hydrodynamic interaction), the short-time behavior of $F(k,t)$ is known to be described by

$$F(k,t) = S(k)e^{-D^{\mathrm{c}}\mathbf{k}^2 t}, \quad D^{\mathrm{c}} = D^{\mathrm{c}}(k) = \frac{D}{S(k)}, \tag{2.10}$$

with D^{c} referred to as the (short-time) collective diffusion coefficient [48]. To be consistent with Eq. (2.10), the coefficient of the linear term of the Dean-Kawasaki equation in the Fourier representation must be $-D^{\mathrm{c}}\mathbf{k}^2$.

For later convenience, we define

$$\ell_0 = \frac{L}{N^{1/n_{\mathrm{d}}}} = \begin{cases} 1/\rho_0 & (n_{\mathrm{d}} = 1) \\ 1/\sqrt{\rho_0} & (n_{\mathrm{d}} = 2)\,, \end{cases} \tag{2.11}$$

which is on the order of the typical distance between the centers of the neighboring particles.

III. DISPLACEMENT CORRELATION TENSOR

For the system of colloidal particles specified in the previous section and governed by Eq. (2.1), now let us devise a statistical quantity which is at once indicative of the cooperative motion and amenable to analytical calculation. The quantity of our choice for it is the displacement correlation tensor.

A. Definition

Let us consider $\mathbf{R}_i(t,s)$ defined in Eq. (1.1); or $\mathbf{R}_i(t) = \mathbf{r}_i(t) - \mathbf{r}_i(0)$, which suffices if the system is statistically steady. We denote the Cartesian components of $\mathbf{R}_i$, in the 2D setup, with

$$\mathbf{R}_i = \begin{bmatrix} R_{i1} \\ R_{i2} \end{bmatrix}, \tag{3.1}$$

omitting the time arguments when obvious. The tensorial product of $\mathbf{R}_i$ and $\mathbf{R}_j$ has four components, which could be expressed in a matrix form, as

$$\mathbf{R}_i \otimes \mathbf{R}_j = \begin{bmatrix} R_{i1}R_{j1} & R_{i1}R_{j2} \\ R_{i2}R_{j1} & R_{i2}R_{j2} \end{bmatrix}. \tag{3.2}$$

Our target is the *displacement correlation tensor*,

$$\mathsf{X}(\tilde{\mathbf{d}},t) = \langle \mathbf{R} \otimes \mathbf{R}\rangle_{\tilde{\mathbf{d}}} = \begin{bmatrix} \langle R_1 R_1\rangle_{\tilde{\mathbf{d}}} & \langle R_1 R_2\rangle_{\tilde{\mathbf{d}}} \\ \langle R_2 R_1\rangle_{\tilde{\mathbf{d}}} & \langle R_2 R_2\rangle_{\tilde{\mathbf{d}}} \end{bmatrix}, \tag{3.3}$$

where $\langle\ \ \rangle_{\tilde{\mathbf{d}}}$ denotes conditional averaging over the pairs of particles (i,j) whose relative position vector at the initial time equals $\tilde{\mathbf{d}}\,(\neq \mathbf{0})$. If the initial time is taken at $t = 0$, the condition is expressed as follows: the initial value of the relative position vector, $\mathbf{r}_{ij}^{\mathrm{init}} = \mathbf{r}_j(0) - \mathbf{r}_i(0)$, should be equal to $\tilde{\mathbf{d}}$. The symbol $\mathsf{X}(\tilde{\mathbf{d}},t)$ with the arguments $(\tilde{\mathbf{d}},t)$ is used in order to make it clear that the displacement correlation tensor in Eq. (3.3) is a function of the initial distance $\tilde{\mathbf{d}}$ and the time interval t. The conditional averaging can be reexpressed as [54]

$$\mathsf{X}(\tilde{\mathbf{d}},t) = \frac{L^{n_{\mathrm{d}}}}{N^2}\left\langle \sum_{i,j} \frac{\delta^{n_{\mathrm{d}}}\left(\mathbf{r}_{ij}^{\mathrm{init}} - \tilde{\mathbf{d}}\right)}{g_2\left(\mathbf{r}_{ij}^{\mathrm{init}}\right)} \mathbf{R}_i \otimes \mathbf{R}_j \right\rangle, \tag{3.4}$$

where

$$g_2(\mathbf{r}) = \frac{L^{n_{\mathrm{d}}}}{N^2}\left\langle \sum_{i',j'} \delta^{n_{\mathrm{d}}}(\mathbf{r}_{j'} - \mathbf{r}_{i'} - \mathbf{r}) \right\rangle \quad (\mathbf{r} \neq \mathbf{0}).$$

Note that $\mathsf{X}(\tilde{\mathbf{d}},t)$ is undefined for $|\tilde{\mathbf{d}}| < \sigma$ because the denominator in Eq. (3.4) vanishes. In the 1D setup, the formulation of the problem can be simpler [30,55]. Since we can take it for granted that the particles are numbered consecutively if $V_{\max} \gg k_{\mathrm{B}}T$ [56], it is meaningful to calculate the displacement correlation in the form of $\langle R_i R_j\rangle$ as a function of t and $|j - i|$. In higher dimensions, of course, the meaning of $\langle \mathbf{R}_i \otimes \mathbf{R}_j\rangle$ is not clear unless the way of numbering is specified, and therefore $\mathsf{X}(\tilde{\mathbf{d}},t)$ must be used instead.

For the sake of simplicity, when the distinction in regard to the independent variable is not important, we may denote both $\mathsf{X}(\tilde{\mathbf{d}},t)$ and $\langle R_i R_j\rangle$ symbolically with $\langle \mathbf{R} \otimes \mathbf{R}\rangle$.

B. Numerical demonstration of vortical motion

As a pictorial representation of the vortical cooperative motion, we plot the numerical value of

$$\mathsf{X}(\tilde{\mathbf{d}},t) \cdot \mathbf{e}_1 = \begin{bmatrix} \langle R_1 R_1\rangle_{\tilde{\mathbf{d}}} \\ \langle R_2 R_1\rangle_{\tilde{\mathbf{d}}} \end{bmatrix}$$

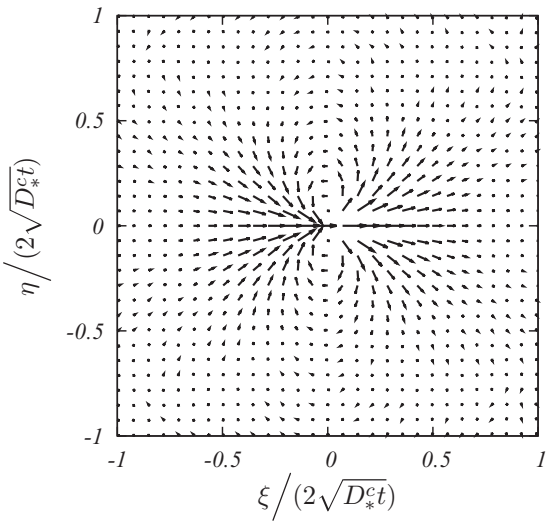

FIG. 1. Displacement correlation in the 2D system ($\phi = 0.5$). The numerical value of $\mathsf{X}(\tilde{\mathbf{d}},t)\cdot\mathbf{e}_1$, computed for $t = 0.8$, is plotted as a vector field on the $\tilde{\mathbf{d}}$ plane.

as a vector field on the $\tilde{\mathbf{d}}$ plane, where $\mathbf{e}_1$ is the x-directional unit vector. The result is shown in Fig. 1. It demonstrates basically the same flow structure as in Fig. 8 of Doliwa and Heuer [5], with a pair of vortices.

The displacement correlation is computed on the assumption that the system is statistically steady, homogeneous, and isotropic and also has the reflectional symmetry. Due to these symmetries (as is well-known in the theory of homogeneous turbulence [13–15]), the displacement correlation tensor must be expressible in the form

$$\mathsf{X}(\tilde{\mathbf{d}},t) = X_\parallel(\tilde{d}/\ell_0,t)\frac{\tilde{\mathbf{d}}\otimes\tilde{\mathbf{d}}}{\tilde{\mathbf{d}}^2} + X_\perp(\tilde{d}/\ell_0,t)\left(\mathbb{1} - \frac{\tilde{\mathbf{d}}\otimes\tilde{\mathbf{d}}}{\tilde{\mathbf{d}}^2}\right), \tag{3.5}$$

where $\tilde{d} = |\tilde{\mathbf{d}}|$. The longitudinal and transverse correlations are denoted with $X_\parallel$ and $X_\perp$, respectively. The positional arguments of these functions are scaled with ℓ_0 for later convenience. In the numerical calculation, $X_\parallel$ and $X_\perp$ are evaluated by decomposing $\mathbf{R}_i$ and $\mathbf{R}_j$ in Eq. (3.4) into the components parallel and perpendicular to $\mathbf{r}_{ij}^{\rm init}$ and then averaging their products with a method similar to the one explained in the Appendix A of Ref. [30]. The average was typically taken over 9600 samples with independent initial conditions.

We emphasize that the displacement correlation, $\langle\mathbf{R}\otimes\mathbf{R}\rangle$, is a two-time statistical quantity involving four points in the space-time. One may question whether such a complicated quantity is necessary, because it seems possible to capture vortical motions by means of one-time correlation of the velocity field, as is the case in fluid or granular turbulence [10,12]. Unfortunately, due to the Langevin noise that breaks the momentum conservation, the velocity field in the colloidal liquid is so noisy that its simple spatial correlation does not provide useful information. In other words, the Langevin noise disqualifies the momentum (and the velocity) for treatment as a slow variable; this is why a two-time quantity $\mathbf{R}$ must be used instead of the instantaneous velocity.

One may notice, by careful observation, a subtle difference between Fig. 1 in the present paper and Fig. 8 of Doliwa and Heuer [5]: the former is symmetric in regard to reflection along the x axis, while the latter appears somewhat asymmetric. This disagreement seems to have originated from the different ways to incorporate the directionality of the "central" particle. Doliwa and Heuer [5] produced their Fig. 8 by averaging the direction of $\mathbf{R}_j$ for all the pairs (i,j), on the condition that the whole system is turned so that $\mathbf{R}_i$ points in the *positive* direction of the x axis. On the other hand, Eq. (3.5) is invariant under replacement of $\tilde{\mathbf{d}}$ with $-\tilde{\mathbf{d}}$, which means that our definition incorporates displacements both *parallel* and *antiparallel* to $\tilde{\mathbf{d}}$ with equal weightings. In this sense, due to the present definition of $\langle\mathbf{R}\otimes\mathbf{R}\rangle$ which is simpler than the procedure in Ref. [5], some information might be lost. Nevertheless, the present definition is advantageous to analytical calculation, as will be seen in the next section. The asymmetry would be captured by a higher-order correlation such as $\langle|\mathbf{R}_i - \mathbf{R}_j|^2(\mathbf{R}_i - \mathbf{R}_j)\rangle$, which we leave as a future work.

IV. ANALYTICAL CALCULATION OF DISPLACEMENT CORRELATION TENSOR

In what follows, we outline the procedure for analytical calculation of $\langle\mathbf{R}\otimes\mathbf{R}\rangle$, developed by the group of the present authors [30,31,55] with the label variable method [57]. The idea is clarified in the 1D setup and then applied to the 2D case.

A. One-dimensional theory

As was pointed out by Doliwa and Heuer themselves [5], the phenomenon of a growing dynamical length scale is exhibited by simpler systems, like a 1D chain of N diffusive particles connected by harmonic springs, as described by the Langevin equation

$$\mu\dot{X}_i = \kappa(X_{i+1} - 2X_i + X_{i-1}) + \mu f_i(t) \tag{4.1}$$

with κ denoting the effective spring constant [58,59]. This is also known as the Rouse model in the context of polymer dynamics [60].

For the system described by Eq. (4.1), where X_i denotes the position of the ith particle numbered consecutively, the displacement correlation is obtained analytically [30,61]. Taking the continuous limit for simplicity, we rewrite Eq. (4.1) in terms of $h = h(\xi,t) = x(\xi,t) - \ell_0\xi$, with ξ here denoting a continuum analog of i, and with ℓ_0 defined in Eq. (2.11). The equation for h reads

$$\partial_t h(\xi,t) = D'\partial_\xi^2 h(\xi,t) + f_h(\xi,t), \tag{4.2}$$

where $D' = \kappa/\mu$, and f_h is a thermal noise such that

$$\langle f_h(\xi,t) f_h(\xi',t')\rangle = 2D\delta(\xi - \xi')\delta(t - t').$$

Since Eq. (4.2) is readily solved in the Fourier representation, various statistical quantities can be calculated analytically. In particular, by noticing that the displacement of the particle labeled with ξ is given by

$$R(\xi,t,s) = x(\xi,t) - x(\xi,s) = h(\xi,t) - h(\xi,s), \tag{4.3}$$

the displacement correlation is obtained in the form

$$\frac{\langle R(\xi,t,s)R(\xi',t,s)\rangle}{\sqrt{D'(t-s)}} \propto \varphi(\theta) \tag{4.4}$$

in terms of the similarity variable $\theta = (\xi - \xi')/\lambda(t-s)$, where $\lambda(t-s) \propto \sqrt{t-s}$ is the dynamical correlation length that diverges to infinity for $t - s \to +\infty$.

Recently the group of the present authors succeeded in extending the above analysis to colloidal systems modeled by the Dean-Kawasaki equation (2.6) [30,31,55]. One of the key ideas is to introduce the variable ξ, referred to as the *label variable*, not through consecutive numbering of the particles but through the equation

$$(\rho, Q) = \begin{vmatrix} \mathbf{e}_0 & \partial_t \xi \\ \mathbf{e}_1 & \partial_x \xi \end{vmatrix} = (\partial_x \xi,\ -\partial_t \xi), \tag{4.5}$$

where $\mathbf{e}_0$ and $\mathbf{e}_1$ are the unit vectors along the t axis and the x axis of the $1+1$-dimensional space-time. It is readily shown, by taking the inner product of (ρ, Q) in Eq. (4.5) and $(\partial_t \xi, \partial_x \xi)$, that $\xi = \xi(x,t)$ satisfies the convective equation,

$$\rho(\partial_t + u\partial_x)\xi(x,t) = 0,$$

where u is the velocity field such that $Q = \rho u$. It implies that specifying a constant value of $\xi(x,t)$ works as a label for the worldline of a particle, hence the name *label variable*. The mapping from x to ξ is then inverted, as

$$\xi \mapsto x = x(\xi,t), \tag{4.6}$$

so that ξ is hereafter treated as an independent variable. Note that this inversion would be highly singular if the delta function in Eq. (2.4) were not blunted; in actuality, this singularity is mitigated as a consequence of the coarse graining. Another crucial idea consists in adoption of the field variable ψ, as a link between the density field and the displacement correlation. The variable ψ is defined by the relation

$$\partial_\xi x(\xi,t) = \ell_0[1 + \psi(\xi,t)]; \tag{4.7}$$

as the expression on the left-hand side equals $1/\rho$ due to Eq. (4.5), ψ can be interpreted as elongation of the particle interval [57,62]. The adoption of ψ as the field variable corresponds to the vacancy-based description of 1D lattice gases [63,64]. In terms of the Fourier representation of ψ, defined as

$$\check{\psi}(k,t) = \frac{1}{N}\int e^{\mathrm{i}k\xi}\psi(\xi,t)\,d\xi \quad \left(\frac{k}{2\pi/N} \in \mathbb{Z}\right) \tag{4.8}$$

so that

$$\psi(\xi,t) = \sum_k \check{\psi}(k,t)e^{-\mathrm{i}k\xi}, \tag{4.9}$$

we consider the two-time correlation

$$C(k,t,s) = \frac{N}{L^2}\langle \check{\psi}(k,t)\check{\psi}(-k,s)\rangle; \tag{4.10}$$

if the system is statistically steady, then it suffices to consider $C(k,t') = C(k,s+t',s)$. Using the Fourier representation in Eq. (4.9) and the relation

$$\partial_\xi R(\xi,t,s) = \ell_0[\psi(\xi,t) - \psi(\xi,s)] \tag{4.11}$$

derived from Eq. (4.7), we can construct a formula that gives the displacement correlation in terms of C in Eq. (4.10). In the case of statistically steady systems, the formula reads

$$\langle R(\xi,t)R(\xi',t)\rangle = \frac{L^4}{\pi N^2}\int_{-\infty}^{\infty} e^{-\mathrm{i}k(\xi-\xi')}\frac{C(k,0)-C(k,t)}{k^2}\,dk, \tag{4.12}$$

where $R(\xi,t) = x(\xi,t) - x(\xi,0)$; Eq. (4.12), as well as its extensions, is referred to as the Alexander-Pincus formula, named after the authors of a celebrated work on single-file diffusion [65].

We note that Eq. (4.12) can be inverted into the form that gives $[C(k,0) - C(k,t)]/k^2$ in terms of the displacement correlation. This form will be discussed later in Sec. IV D, together with its 2D analogs, as the "inverse" of our present strategy: we are targeting at $\langle \mathbf{R} \otimes \mathbf{R}\rangle$ by means of the Alexander-Pincus formula, into which we need C as an input.

In order to calculate C, we rewrite the Dean-Kawasaki equation by changing the independent variables from (x,t) to (ξ,t) [30,57,66]. The continuity equation (2.5) is replaced by

$$\ell_0 \partial_t \psi(\xi,t) = \partial_\xi u(\xi,t) \tag{4.13}$$

in the 1D case, and we substitute $u = Q/\rho$ into Eq. (4.13) where Q is given by the 1D version of Eq. (2.6). Switching to the Fourier representation in terms of $\check{\psi}$, we have

$$\partial_t \check{\psi}(k,t) = -D^{\mathrm{c}}_* k^2 \check{\psi}(k,t) + O(\check{\psi}^2) + \rho_0 \check{f}_{\mathrm{L}}(k,t) \tag{4.14}$$

with the statistics of the random force term given as

$$\rho_0^2\langle \check{f}_{\mathrm{L}}(k,t)\check{f}_{\mathrm{L}}(-k',t')\rangle = \frac{2D_*}{N}k^2\delta_{kk'}\delta(t-t'); \tag{4.15}$$

here we have defined $D_* = D/\ell_0^2$ and $D^{\mathrm{c}}_* = D^{\mathrm{c}}/\ell_0^2$, with $D^{\mathrm{c}} = D^{\mathrm{c}}(k)$ denoting the collective diffusion coefficient in Eq. (2.10) at the label-space wave number k (physical wavelength $2\pi\ell_0/k$). Within the linear approximation, Eq. (4.14) readily yields

$$C(k,t) = \frac{S(k)}{L^2}e^{-D^{\mathrm{c}}_* k^2 t}, \tag{4.16}$$

which is substituted into the Alexander-Pincus formula (4.12). Since the contribution from the long-wave modes is dominant, the k dependence of $S(k) \simeq S(0) + O(k^2)$ can be ignored, and D^{c}_* is also regarded as independent of k. Then, upon evaluation of the integral, we obtain

$$\frac{\langle R(\xi,t)R(\xi',t)\rangle}{\sigma\sqrt{D^{\mathrm{c}}t}} = \frac{2S}{\rho_0\sigma}\left(\frac{e^{-\theta^2}}{\sqrt{\pi}} - |\theta|\,\mathrm{erfc}\,|\theta|\right) = \varphi(\theta), \tag{4.17}$$

in terms of a similarity variable, $\theta = (\xi - \xi')/\lambda(t)$, with the dynamical correlation length $\lambda(t) = 2\sqrt{D^{\mathrm{c}}t}$. This is evidently in the form of Eq. (4.4).

The function φ in Eq. (4.17) is plotted in Fig. 2. To emphasize the vectorial character of the displacement, the 1D

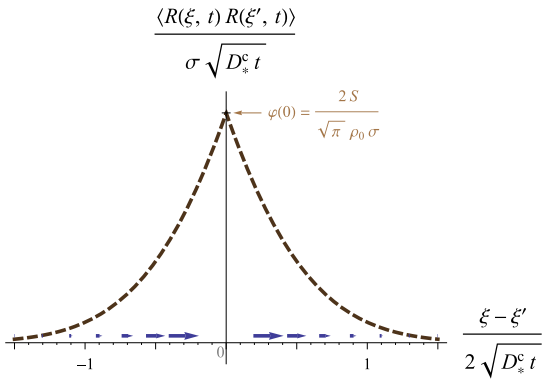

FIG. 2. Displacement correlation in the 1D case, given in Eq. (4.17).

vector field

$$\frac{\langle \mathbf{R}(\xi,t)\otimes\mathbf{R}(0,t)\rangle}{\sigma\sqrt{D^{c}t}}\cdot\mathbf{e}_1=\varphi\left(\frac{\xi}{\lambda(t)}\right)\mathbf{e}_1$$

is shown together; this might be interpreted as illustrating the average collective motion of the particles, on the condition that the central particle has moved rightward.

A nonlinear theory can be developed by taking into account the quadratic nonlinear terms that are ignored in Eq. (4.14), in the form of mode-coupling theory (MCT) for $C(k,t)$ [30]. The notorious difficulty concerning the violation of the fluctuation-dissipation theorem is naturally resolved by the choice of the variable, namely $\psi(\xi,t)$ instead of $\rho(x,t)$. Although there are an infinite number of nonlinear terms in the power series for the ideal solution entropy, $\log(1+\psi)=\psi-\psi^2/2+\cdots$, we truncated the series focusing on the long-time behavior, with the exponential decay in Eq. (4.16) in mind; this treatment is numerically justified by asymptotic validity of the linear result in Eq. (4.17). The memory integral in the MCT equation gives a correction to $C(k,t)$ in Eq. (4.16), resulting in modification of Eq. (4.17) as

$$\langle R(\xi,t)R(\xi',t)\rangle=\sigma\sqrt{D^{c}t}\,\varphi(\theta)-\frac{\sqrt{2}}{3\pi}\ell_0^2(1-2\theta^2)e^{-\theta^2}. \tag{4.18}$$

The correction term is shown to have a perceptible effect on the mean square displacement (MSD), i.e., the short-length limit of the displacement correlation, in regard to its finite-time behavior [30,31,67].

The displacement correlation can be regarded as generalization of MSD to the two-particle statistics and is related to another form of two-particle two-time correlation, $\langle[x(\xi,t)-x(\xi',0)]^2\rangle$ in our notation. Information of the interparticle distance correlation [58], regardable as an analog of bond breaking [2,68,69], is also contained in this form of correlation. Recently the probability distribution function corresponding to this correlation was shown to be calculable exactly in the special case of the 1D system of point particles [70]. Instead of going into details of 1D systems, however, we will now focus on the problem of how to proceed to the 2D case.

B. Relation between the initial position and the label variable

As was remarked at the end of Sec. III A, we have sometimes denoted the displacement correlation symbolically as $\langle\mathbf{R}\otimes\mathbf{R}\rangle$, without specifying the independent variable. This is not a serious problem when the consecutive numbering or its continuum limit provides a natural choice of the independent variable, as is the case in the 1D system.

Before proceeding to the 2D theory, however, the relation between the label variable, ξ, and the initial position of the particle, $x^{\rm init}=x(\xi,0)$, should be briefly discussed. In general, there is a certain degree of freedom in definition of the label variable. At the hydrodynamic scale where continuum description is valid in the usual sense, the label variable should be a smooth one-to-one function of the initial position. A popular choice is to select the identity function, so that $\xi=x^{\rm init}$, or to define $\xi=x^{\rm init}/\ell_0$ if ξ is desired to be nondimensional. However, we have not made this naive choice.

Our definition of the label variable in Eq. (4.5) is devised so as to reproduce the particle numbering in the 1D setup. It allows for the density fluctuation at $t=0$, as is seen from Eq. (4.7), which implies

$$x_{\rm B}^{\rm init}-x_{\rm A}^{\rm init}=\ell_0\int_{\rm A}^{\rm B}[1+\psi(\xi,0)]\,d\xi \tag{4.19}$$

for the initial distance between the particles A and B. Due to the presence of ψ on the right-hand side of Eq. (4.19), $\xi_{\rm B}-\xi_{\rm A}$ differs from $(x_{\rm B}^{\rm init}-x_{\rm A}^{\rm init})/\ell_0$ in general. However, since the integral of ψ tends to average out to zero for large distance, we may expect

$$\frac{x_{\rm B}^{\rm init}-x_{\rm A}^{\rm init}}{\ell_0}\simeq\xi_{\rm B}-\xi_{\rm A} \tag{4.20}$$

as an *approximate* relation. This approximation also justifies assuming $C(k,0)\simeq S(0)/L^2$ for small k, even if nonlinearity is taken into account.

If we accept Eq. (4.20), the displacement correlation as a function of $\tilde{d}$ and t, $\mathsf{X}(\tilde{d},t)=X_{\rm 1D}(\tilde{d},t)\mathbf{e}_1\otimes\mathbf{e}_1$, is approximated as

$$X_{\rm 1D}(\tilde{d},t)\simeq\langle R(\xi,t)R(\xi',t)\rangle|_{\xi=\xi'+\tilde{d}/\ell_0}. \tag{4.21}$$

The validity of this approximation can be established by rewriting the 1D version of Eq. (3.4) in the form of an integral over the initial position (see Sec. V-A in Ref. [30]). After some calculation, $X_{\rm 1D}(\tilde{d},t)$ is found to be expressible as a sum of two parts: the first part simply gives Eq. (4.21), while the second part involves triple correlations. The contribution from these triple correlation terms is shown to be asymptotically negligible for large t. In this sense, it is acceptable to identify the label distance $\xi-\xi'$ with the initial distance $\tilde{d}$ divided by ℓ_0, at least as a crude approximation. The approximation should be better for larger distance in space or time.

C. Two-dimensional theory

The procedure for calculation of $\langle\mathbf{R}\otimes\mathbf{R}\rangle$ for 2D colloidal liquids [31] is essentially parallel to its 1D prototype. The starting point is the Dean-Kawasaki equation, written in the form of Eq. (2.6) combined with the continuity equation (2.5). Subsequently, we introduce the label variable $\boldsymbol{\xi}=(\xi,\eta)$ through the 2D analog of Eq. (4.5); we define also the tensorial

field variable Ψ, which is essentially the deformation gradient tensor [71], by generalizing Eq. (4.7) to the 2D case. By calculating the two-time correlations of the components of Ψ, in the Fourier representation, and substituting them into the 2D version of the Alexdander-Pincus formula, we obtain $\mathsf{X}(\tilde{\mathbf{d}},t)$.

In comparison to the 1D case, there are two main differences: first, various quantities appearing in the theory are now tensorial, and second, we cannot depend on the consecutive numbering of the particles. For a pair of particles labeled with $\boldsymbol{\xi}$ and $\boldsymbol{\xi}'$, we expect $\tilde{\mathbf{d}}/\ell_0 \simeq \boldsymbol{\xi} - \boldsymbol{\xi}'$ for the initial relative position vector $\tilde{\mathbf{d}}$, and therefore

$$\mathsf{X}(\tilde{\mathbf{d}},t) \simeq \begin{bmatrix} \langle R_1(\tilde{\mathbf{d}}/\ell_0,t)R_1(\mathbf{0},t)\rangle & \langle R_1(\tilde{\mathbf{d}}/\ell_0,t)R_2(\mathbf{0},t)\rangle \\ \langle R_2(\tilde{\mathbf{d}}/\ell_0,t)R_1(\mathbf{0},t)\rangle & \langle R_2(\tilde{\mathbf{d}}/\ell_0,t)R_2(\mathbf{0},t)\rangle \end{bmatrix}, \tag{4.22}$$

where we have chosen $\boldsymbol{\xi}' = \mathbf{0}$ without loss of generality, assuming translational invariance. As we further assume rotational and reflectional invariance of the system, $\mathsf{X}(\tilde{\mathbf{d}},t)$ must be expressed in the form of Eq. (3.5) as a sum of the longitudinal and the transverse components, represented by two functions, namely, $X_\parallel(|\boldsymbol{\xi}|,t)$ and $X_\perp(|\boldsymbol{\xi}|,t)$. The goal of the calculation is to obtain analytical expressions for these two functions.

The procedure of the calculation starts with introducing the label variable $\boldsymbol{\xi} = (\xi,\eta)$ and thereby rewriting the Dean-Kawasaki equation (2.6). Recalling that Eq. (4.5) relates ξ to (ρ, Q), we introduce $\boldsymbol{\xi} = (\xi,\eta)$ as a solution to the equation

$$(\rho,\mathbf{Q}) = \begin{vmatrix} \mathbf{e}_0 & \partial_t\xi & \partial_t\eta \\ \mathbf{e}_1 & \partial_x\xi & \partial_x\eta \\ \mathbf{e}_2 & \partial_y\xi & \partial_y\eta \end{vmatrix}. \tag{4.23}$$

Then $\boldsymbol{\xi}$ is demonstrated to satisfy the convective equation and thus qualified as the label variable. Note that an extension to the three-dimensional (3D) case is straightforward, and the cofactor expansion reproduces the equations suggested in Ref. [57].

The mapping from the label variable to the position,

$$\boldsymbol{\xi} = (\xi,\eta) \mapsto \mathbf{r}(\boldsymbol{\xi},t) = \begin{bmatrix} x(\xi,\eta,t) \\ y(\xi,\eta,t) \end{bmatrix}, \tag{4.24}$$

specifies a time-dependent curvilinear coordinate system which is sometimes referred to as the *convected coordinate system* [72,73]. The time derivative of $\mathbf{r}(\boldsymbol{\xi},t)$ gives the velocity, $\mathbf{u} = \partial_t\mathbf{r}(\boldsymbol{\xi},t)$. The "spatial" derivative gives what is called the deformation gradient tensor [71] or the displacement gradient tensor [72]. Thereby we define Ψ as

$$\begin{bmatrix} \partial_\xi x & \partial_\eta x \\ \partial_\xi y & \partial_\eta y \end{bmatrix} = \ell_0(\mathbb{1} + \Psi), \tag{4.25}$$

which is intended as the 2D generalization of Eq. (4.7). Out of the four components of Ψ, only two are independent. If we choose the diagonal components of Ψ to represent them, as

$$\Psi = \begin{bmatrix} \Psi_1 & \partial_\eta\partial_\xi^{-1}\Psi_1 \\ \partial_\xi\partial_\eta^{-1}\Psi_2 & \Psi_2 \end{bmatrix}, \tag{4.26}$$

and introduce their Fourier modes by

$$\begin{bmatrix} \Psi_1(\boldsymbol{\xi},t) \\ \Psi_2(\boldsymbol{\xi},t) \end{bmatrix} = \sum_{\mathbf{k}} \begin{bmatrix} \check{\Psi}_1(\mathbf{k},t) \\ \check{\Psi}_2(\mathbf{k},t) \end{bmatrix} e^{-i\mathbf{k}\cdot\boldsymbol{\xi}}, \tag{4.27}$$

the Dean-Kawasaki equation (2.6) is rewritten as

$$\partial_t \begin{bmatrix} \check{\Psi}_1(\mathbf{k},t) \\ \check{\Psi}_2(\mathbf{k},t) \end{bmatrix} = -D_*^{\mathrm{c}} \begin{bmatrix} k_1^2 & k_1^2 \\ k_2^2 & k_2^2 \end{bmatrix} \begin{bmatrix} \check{\Psi}_1(\mathbf{k},t) \\ \check{\Psi}_2(\mathbf{k},t) \end{bmatrix} + O(\Psi^2) + \ell_0^{-1} \begin{bmatrix} \check{f}_1(\mathbf{k},t) \\ \check{f}_2(\mathbf{k},t) \end{bmatrix}; \tag{4.28}$$

the forcing statistics are given by

$$\ell_0^{-2} \begin{bmatrix} \langle \check{f}_1(\mathbf{k},t)\check{f}_1(-\mathbf{k}',t')\rangle & \langle \check{f}_1(\mathbf{k},t)\check{f}_2(-\mathbf{k}',t')\rangle \\ \langle \check{f}_2(\mathbf{k},t)\check{f}_1(-\mathbf{k}',t')\rangle & \langle \check{f}_2(\mathbf{k},t)\check{f}_2(-\mathbf{k}',t')\rangle \end{bmatrix} = \frac{2D_*}{N} \begin{bmatrix} k_1^2 & 0 \\ 0 & k_2^2 \end{bmatrix} \delta_{\mathbf{k},\mathbf{k}'}\delta(t-t'), \tag{4.29}$$

with $D_* = D/\ell_0^2 = \rho_0 D$. The factor $\delta_{\mathbf{k},\mathbf{k}'}$ originates from the random distribution of the particles, which should be uniform for small values of $\mathbf{k}$.

The linear homogenous part of Eq. (4.28) has two eigenvalues: $-D_*^{\mathrm{c}}\mathbf{k}^2$ and 0. Accordingly, we diagonalize Eq. (4.28) by reexpressing $(\check{\Psi}_1, \check{\Psi}_2)$ as a linear combination of the eigenvectors. This diagonalization corresponds to switching to the dilatational and rotational modes, denoted with ψ_{d} and ψ_{r}, respectively, and defined as

$$\partial_\xi x + \partial_\eta y = \ell_0\left(2 + \sum_{\mathbf{k}} \psi_{\mathrm{d}}(\mathbf{k},t)e^{-i\mathbf{k}\cdot\boldsymbol{\xi}}\right), \tag{4.30}$$

$$\partial_\xi y - \partial_\eta x = \ell_0 \sum_{\mathbf{k}} \psi_{\mathrm{r}}(\mathbf{k},t)e^{-i\mathbf{k}\cdot\boldsymbol{\xi}}. \tag{4.31}$$

The correlations of these modes are denoted by

$$C_{ab}(\mathbf{k},t,s) = \frac{N}{L^4}\langle \psi_a(\mathbf{k},t)\psi_b(-\mathbf{k},s)\rangle \tag{4.32}$$

with $a,b \in \{\mathrm{d},\mathrm{r}\}$ and $s < t$. In the present case, however, C_{rd} is found to vanish, and for the sake of brevity, we write C_{d} for C_{dd} and C_{r} for C_{rr}, respectively. The linearized equation yields

$$C_{\mathrm{d}}(\mathbf{k},t,s) = \frac{S}{L^4}e^{-D_*^{\mathrm{c}}\mathbf{k}^2(t-s)}, \tag{4.33a}$$

$$C_{\mathrm{r}}(\mathbf{k},t,s) = \frac{2D_*\mathbf{k}^2}{L^4}(s-o), \tag{4.33b}$$

where o is a constant of integration, interpretable as the time at which C_{r} is reset. Note that both C_{d} and C_{r} are independent of the direction of $\mathbf{k}$.

From C_{d} and C_{r} in Eq. (4.33), the displacement correlation is obtained via the Alexander-Pincus formula [31], which now reads

$$\begin{bmatrix} \langle R_1(\boldsymbol{\xi},t,s)R_1(\mathbf{0},t,s)\rangle & \langle R_1(\boldsymbol{\xi},t,s)R_2(\mathbf{0},t,s)\rangle \\ \langle R_2(\boldsymbol{\xi},t,s)R_1(\mathbf{0},t,s)\rangle & \langle R_2(\boldsymbol{\xi},t,s)R_2(\mathbf{0},t,s)\rangle \end{bmatrix} = \frac{L^6}{2\pi^2 N}\iint \left[\frac{C_{\mathrm{d}}(\mathbf{k},s,s)+C_{\mathrm{d}}(\mathbf{k},t,t)}{2} - C_{\mathrm{d}}(\mathbf{k},t,s)\right] \times \begin{bmatrix} k_1^2 & k_1k_2 \\ k_2k_1 & k_2^2 \end{bmatrix} \frac{e^{-i\mathbf{k}\cdot\boldsymbol{\xi}}}{\mathbf{k}^4}\, dk_1\, dk_2$$

$$+\frac{L^6}{2\pi^2 N}\iint\left[\frac{C_{\rm r}(\mathbf{k},s,s)+C_{\rm r}(\mathbf{k},t,t)}{2}-C_{\rm r}(\mathbf{k},t,s)\right]\times\begin{bmatrix}k_2^2 & -k_1k_2\\ -k_2k_1 & k_1^2\end{bmatrix}\frac{e^{-i\mathbf{k}\cdot\boldsymbol{\xi}}}{\mathbf{k}^4}\,dk_1\,dk_2. \tag{4.34}$$

Equation (4.33a) gives

$$\frac{C_{\rm d}(\mathbf{k},s,s)+C_{\rm d}(\mathbf{k},t,t)}{2}-C_{\rm d}(\mathbf{k},t,s)=\frac{S}{L^4}\left[1-e^{-D_*^{\rm c}\mathbf{k}^2(t-s)}\right] \tag{4.35}$$

for the integrand in the first term on the right-hand side of Eq. (4.34), while the corresponding expression in the second term is calculated as

$$\frac{C_{\rm r}(\mathbf{k},s,s)+C_{\rm r}(\mathbf{k},t,t)}{2}-C_{\rm r}(\mathbf{k},t,s)=\frac{D_*\mathbf{k}^2}{L^4}(t-s) \tag{4.36}$$

from Eq. (4.33b). The integrals are then evaluated and the result is equated to $\mathsf{X}(\tilde{\mathbf{d}},t)$ in Eq. (3.5), which yields

$$X_\parallel(|\boldsymbol{\xi}|,t)=\frac{S}{4\pi\rho_0}\left[E_1(\theta^2)+\frac{e^{-\theta^2}}{\theta^2}\right], \tag{4.37a}$$

$$X_\perp(|\boldsymbol{\xi}|,t)=\frac{S}{4\pi\rho_0}\left[E_1(\theta^2)-\frac{e^{-\theta^2}}{\theta^2}\right], \tag{4.37b}$$

where $\boldsymbol{\xi}=(\xi,\eta)\simeq\tilde{\mathbf{d}}/\ell_0$ and

$$\theta^2=\frac{\xi^2+\eta^2}{4D_*^{\rm c}t}\simeq\frac{\tilde{\mathbf{d}}^2}{[\lambda(t)]^2} \tag{4.38}$$

with $\lambda(t)=2\sqrt{D^{\rm c}t}$, and $E_1(\,\cdot\,)$ denotes the exponential integral [74]:

$$E_1(z)=\int_z^\infty\frac{e^{-\zeta}}{\zeta}\,d\zeta. \tag{4.39}$$

Using the asymptotic expansion of $E_1(z)$ for large z, from Eq. (4.37) we find

$$X_\parallel(|\boldsymbol{\xi}|,t)\simeq\frac{S}{4\pi\rho_0}e^{-\theta^2}(2\theta^{-2}-\theta^{-4}+\cdots), \tag{4.40a}$$

$$X_\perp(|\boldsymbol{\xi}|,t)\simeq\frac{S}{4\pi\rho_0}e^{-\theta^2}(-\theta^{-4}+\cdots) \tag{4.40b}$$

for large θ.

D. Inverse of Alexander-Pincus formulas

Our analytical calculation, starting from the Dean-Kawasaki equation, is routed through the Alexander-Pincus formula, into which we input C in Eq. (4.10) or its 2D analogs in Eq. (4.32) to obtain $\langle\mathbf{R}\otimes\mathbf{R}\rangle$ as the output. It is, however, sometimes convenient to reverse a part of this course.

In the 1D case, the Fourier inversion of the Alexander-Pincus formula (4.12) gives

$$\frac{C(k,0)-C(k,t)}{k^2}=\frac{\rho_0^2}{2L^2}\int e^{ik\xi}\langle R(\xi,t)R(0,t)\rangle\,d\xi=\frac{\rho_0^2}{2L^2N}\sum_{i,j}\langle R_iR_j\rangle e^{ik(j-i)}, \tag{4.41}$$

where we have used the relation $d\xi=\rho\,dx$. Here the data set of the displacement R_i is taken as the input. This form may be convenient when one wishes to analyze the data of displacements from experimental observation of a 1D system of particles or from direct numerical simulation of such a system.

The inversion of Eq. (4.34) is slightly more complicated, as we need to separate $C_{\rm d}$ and $C_{\rm r}$. The inverse formulas read

$$\frac{1}{k^2}\left[\frac{C_{\rm d}(\mathbf{k},s,s)+C_{\rm d}(\mathbf{k},t,t)}{2}-C_{\rm d}(\mathbf{k},t,t)\right]=\frac{\rho_0}{2L^4}\iint e^{i\mathbf{k}\cdot\boldsymbol{\xi}}\langle R^{(\parallel\mathbf{k})}(\boldsymbol{\xi},t,s)R^{(\parallel\mathbf{k})}(\mathbf{0},t,s)\rangle\,d\xi\,d\eta, \tag{4.42}$$

$$\frac{1}{k^2}\left[\frac{C_{\rm r}(\mathbf{k},s,s)+C_{\rm r}(\mathbf{k},t,t)}{2}-C_{\rm r}(\mathbf{k},t,t)\right]=\frac{\rho_0}{2L^4}\iint e^{i\mathbf{k}\cdot\boldsymbol{\xi}}\langle R^{(\perp\mathbf{k})}(\boldsymbol{\xi},t,s)R^{(\perp\mathbf{k})}(\mathbf{0},t,s)\rangle\,d\xi\,d\eta, \tag{4.43}$$

where we have defined

$$R^{(\parallel\mathbf{k})}=\mathbf{e}_\mathbf{k}\cdot\mathbf{R},\quad R^{(\perp\mathbf{k})}=\det(\mathbf{e}_\mathbf{k},\mathbf{R})$$

in terms of $\mathbf{e}_\mathbf{k}=\mathbf{k}/k$.

The expression on the right-hand side of Eq. (4.43) is essentially identical to the quantity studied by Flenner and Szamel [27]. In our notation, this quantity is defined as

$$S_4^\perp(\mathbf{q},t)=\frac{1}{N}\left\langle\sum_{i,j}R_i^{(\perp\mathbf{q})}(t)R_j^{(\perp\mathbf{q})}(t)e^{i\mathbf{q}\cdot\mathbf{r}_{ij}^{\rm init}}\right\rangle, \tag{4.44}$$

where $\mathbf{q}$ is Fourier-conjugate to $\mathbf{r}^{\rm init}$. For the length scales much greater than ℓ_0, the approximation

$$\mathbf{k}\cdot\boldsymbol{\xi}\simeq\mathbf{q}\cdot\mathbf{r}_{ij}^{\rm init},\quad\mathbf{k}=\ell_0\mathbf{q}$$

is valid, which makes the integral on the right-hand side of Eq. (4.43) equal to $S_4^\perp(\mathbf{q},t)$. Similarly, one may define

$$S_4^\parallel(\mathbf{q},t)=\frac{1}{N}\left\langle\sum_{i,j}R_i^{(\parallel\mathbf{q})}(t)R_j^{(\parallel\mathbf{q})}(t)e^{i\mathbf{q}\cdot\mathbf{r}_{ij}^{\rm init}}\right\rangle \tag{4.45}$$

and find it equal to the integral on the right-hand side of Eq. (4.42).

By comparing Eqs. (4.42)–(4.45), we notice that $C_{\rm r}$ and $S_4^\perp$ contain essentially the same information, and also that $C_{\rm d}$ and $S_4^\parallel$ are equivalent. The displacement correlation X contains information for both $C_{\rm r}$ and $C_{\rm d}$. The relation of these correlations to the two-time correlation of density, given by $F(k,t)$ in Eq. (2.9), deserves a comment: F represents the same dilatational motion as $C_{\rm d}$ in effect, but not the rotational motion. This implies that, while the first integral in Eq. (4.34) might be expressible in terms of F within some approximation, the second integral requires information of $C_{\rm r}$ which is not reducible to F.

In regard to $X_\parallel$ and $X_\perp$ in Eq. (3.5), it should be warned that Fourier transforms of $X_\parallel$ and $X_\perp$ differ from $S_4^\parallel$ and $S_4^\perp$. This is naturally understood once the difference between the two types of decomposition are recognized: Eq. (3.5) is based on the orthogonal projection onto $\tilde{\mathbf{d}}$, while the quantities in

Eqs. (4.42)–(4.45) are defined in terms of projection onto the wave number vector.

V. COMPARISON OF NUMERICAL AND ANALYTICAL RESULTS

With the numerical data of 2D displacement correlation illustrated in Fig. 1 and the analytical expressions of $X_\parallel(|\boldsymbol{\xi}|,t)$ and $X_\perp(|\boldsymbol{\xi}|,t)$ in Sec. IV, now let us discuss the validity of the analytical results in Eq. (4.37) by comparing them with the numerically computed values. As was stated in Sec. II in regard to the area fraction ϕ, we focus on the case with $\phi = 0.5$; later, in Sec. VI, the cases of several other values of ϕ will be discussed briefly. For the sake of simplicity, hereafter we write ξ instead of $|\boldsymbol{\xi}|$, when it is not confusing.

As the evaluation of the analytical expressions in Eq. (4.37) requires knowledge of the values of $S = S(k \to +0)$ and $D^c = D^c(k \to +0)$, we begin by computing these values. The static structure factor $S(k)$ for $\phi = 0.5$, computed according to the procedure in Ref. [28], is plotted in Fig. 3. From these data, we obtain $S = S(k \to +0) = 0.16$ by extrapolation, and incidentally, we also find the peak wave number $k_{\rm peak} = 6.3\,\sigma^{-1}$. Numerical values of $F(k,t)$, defined by Eq. (2.9), are computed analogously and plotted in Fig. 4, together with the values from Eq. (2.10) represented by the solid lines. As these values in Fig. 4 are seen to be consistent, D^c is confirmed to be related to S by Eq. (2.10).

With the values of S and D^c thus obtained, we can calculate $X_\parallel$ and $X_\perp$ according to the theoretical predictions in Eq. (4.37) and compare them with the corresponding results of direct numerical simulations. Such a comparison is made in Fig. 5, where the functions $X_\parallel(\xi,t)$ and $X_\perp(\xi,t)$ are plotted against $\xi = |\boldsymbol{\xi}| = \tilde{d}/\ell_0$. Each panel contains four sets of numerical data, corresponding to four different values of the time difference t nondimensionalized with σ^2/D. The thin solid lines, representing the predictions of Eq. (4.37), seem to agree with the computed results for larger values of ξ, i.e., at large distances. As ξ increases, both $X_\parallel(\xi,t)$ and $X_\perp(\xi,t)$ tend to zero, and the numerical data suggest that $|X_\perp|$ is always smaller than $X_\parallel$ and seems to vanish faster than $X_\parallel$ (notice the difference in the scale of the vertical axes); this is consistent

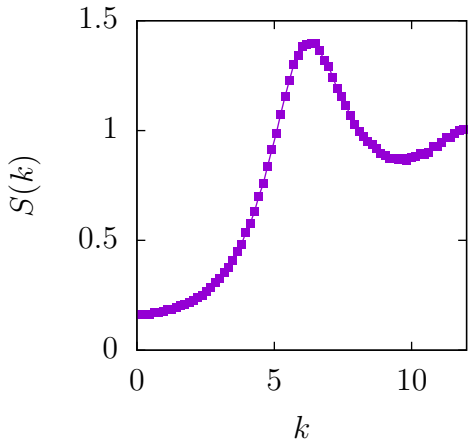

FIG. 3. The static structure factor $S(k)$, computed for $\phi = 0.5$ and giving $S = S(k \to +0) = 0.16$ in this case.

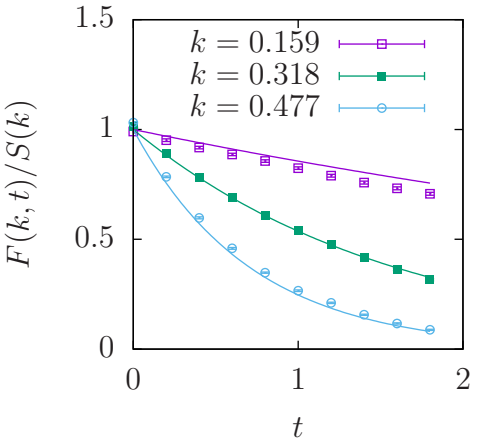

FIG. 4. Temporal decay of $F(k,t)$ for three values of k. Numerical results are shown with points and compared with Eq. (2.10) plotted with the solid lines.

with Eq. (4.37), implying $|X_\perp| < X_\parallel$ for all finite values of ξ, and also with the asymptotic behavior in Eq. (4.40), which can be read as

$$\left|\frac{X_\perp}{X_\parallel}\right| \simeq \frac{1}{2}\theta^{-2} = \frac{[\lambda(t)]^2}{2\xi^2} \ll 1 \tag{5.1}$$

for large ξ.

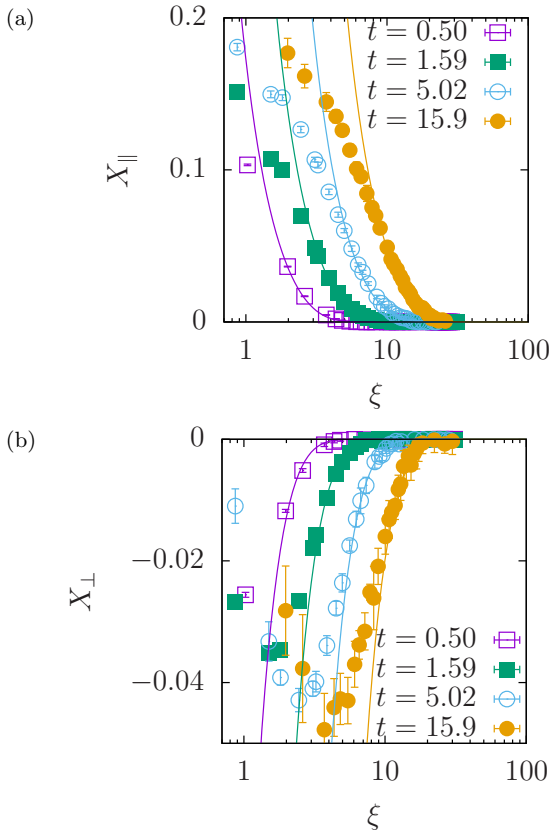

FIG. 5. Numerical values of the longitudinal correlation $X_\parallel(\xi,t)$ and the transverse correlation $X_\perp(\xi,t)$, computed for four different time intervals and plotted against $\xi = |\boldsymbol{\xi}| = \tilde{d}/\ell_0$. The predictions of Eq. (4.37) are shown with thin solid lines.

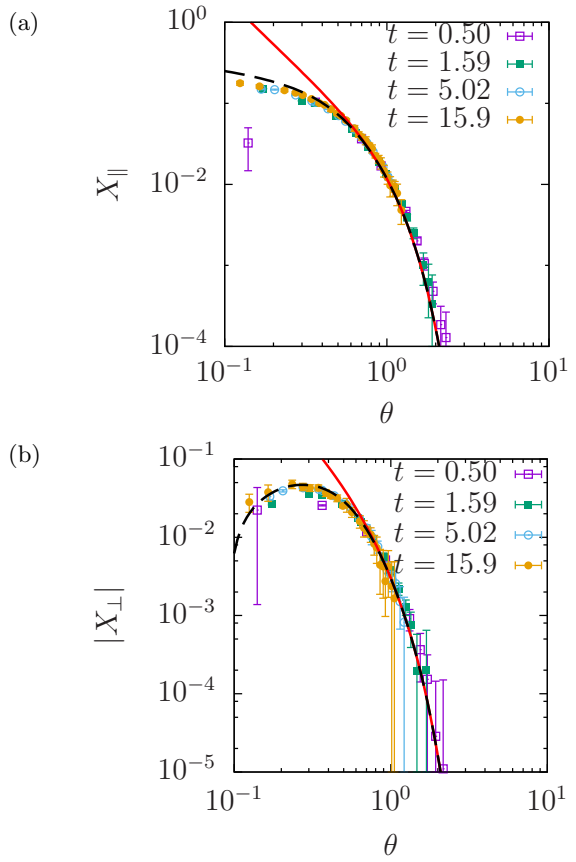

FIG. 6. Verification of Eq. (4.37) by plotting the longitudinal correlation $X_\parallel$ and the transverse correlation $X_\perp$ against the similarity variable $\theta = \ell_0|\boldsymbol{\xi}|/\lambda(t) = |\boldsymbol{\xi}|/(2\sqrt{D_*^{\mathrm{c}}t}\,)$. The solid (red) lines show theoretical predictions in Eq. (4.37), while fitting with Eq. (6.13) is delineated with broken (black) lines.

A striking prediction of Eq. (4.37) that $X_\parallel(\xi,t)$ and $X_\perp(\xi,t)$ will collapse onto master curves, if they are plotted against $\theta = \tilde{d}/\lambda(t)$, is verified in Fig. 6. From the plot of $X_\parallel$ in Fig. 6(a), it is seen that all the four sets of numerical data corresponding to the separate curves in Fig. 5(a) collapse onto a single master curve, and Eq. (4.37a), plotted with a solid (red) line, gives this master curve for $\theta \gtrsim 1$. Besides, the master curve continues to the range of small θ where Eq. (4.37a) is not valid. Analogously, the four data sets in Fig. 5(b) collapse onto a master curve in Fig. 6(b) where $|X_\perp|$ is plotted logarithmically against θ, and the master curve agrees with Eq. (4.37b) for large θ but deviates from it for small θ.

Thus Eq. (4.37) is validated for moderate and large values of θ. Besides, at least in the case of $\phi = 0.5$, $X_\parallel$ and $X_\perp$ are found to be functions of θ alone in the entire range, even if θ is so small that Eq. (4.37) fails.

VI. DISCUSSION

We have calculated displacement correlation tensor both numerically and analytically, which allows us to capture vortical cooperative motion in 2D colloidal liquids. The analytical calculation predicts the cooperative motion to have a self-similar space-time structure, expressible with the similarity variable θ. This prediction has been verified numerically and shown to be quantitatively valid for large θ, corresponding to length scales comparable to and greater than $\lambda(t)$. For shorter scales, the prediction in Eq. (4.37) deviates from the computed result, but it remains true that the numerical data sets for different t collapse onto a single master curve.

As we have stated in the Introduction, these calculations of $\langle \mathbf{R} \otimes \mathbf{R} \rangle$ are intended to prepare the ground for a more elaborate theory of colloidal liquids. Granted that the area fraction in the present study ($\phi = 0.50$) is not large enough to exhibit genuine long-time behavior of colloidal glasses, the present results are already indicative of some precursory features of glassy dynamics. Let us discuss these features, including the longevity of the vortical motion, negative long-time tail in the velocity autocorrelation, and slowdown of C_{r} related to the shear modulus of the liquid.

A. Speculation on caged dynamics

The vortical cooperative motion indicated by $\langle \mathbf{R} \otimes \mathbf{R} \rangle$ is much long-lived, in comparison to the time scale of the structural relaxation (often denoted with τ_α for glassy systems [3,5]), measured by the decay of $F(k,t)$ at the nearest-neighbor distance. In the present case with $\phi = 0.5$, the decay time of $F(k,t)$ at $k = k_{\mathrm{peak}} = 6.3\,\sigma^{-1}$ is smaller than unity (i.e., shorter than σ^2/D in dimensional expression), while the correlations persists to grow until $t = 15.9$ at least, as is attested by Figs. 5 and 6. The mechanism of this (relative) persistence is clarified by Eq. (4.34), in which the integrals are dominated by the long-wave components whose relaxation time diverges as k^{-2} for $k \to 0$. The persistence of the cooperative motion holds also for denser systems studied by Doliwa and Heuer [5], as is exemplified by their Fig. 8 illustrating the vortical motion at $\phi = 0.77$ and $t = 10\tau_\alpha$.

The self-similar behavior of $\langle \mathbf{R} \otimes \mathbf{R} \rangle$, expressible with the similarity variable θ, suggests an onion-like or a matryoshka-like structure, such that the small cages are nested in larger and slower cages [30]. The time scale τ_α signals the start of the cage collapse on the innermost layer of the nested cages, but the outer cage layers survive, though they may be deformed according to the displacement of the central particle. We note that this structure is also observed in the quasi-1D dynamics of Brownian particles (single-file diffusion with overtaking), as is shown in Fig. 4 of Ref. [55], where the overtaking destroys most of the displacement correlation of neighboring particles but there remains very weak positive correlation corresponding to the outer cage layers.

Let us now focus on the central particle confined in the cage structure. Although the short-range behavior of Eq. (4.37) lacks quantitative accuracy, it seems to include an important feature of colloidal systems in regard to the velocity autocorrelation, $\langle \mathbf{u}(t) \cdot \mathbf{u}(s) \rangle$, which is shown to be *negative*. The velocity autocorrelation is a special case of the Lagrangian velocity correlation, $\langle \mathbf{u}(\boldsymbol{\xi},t) \otimes \mathbf{u}(\boldsymbol{\xi}',s) \rangle$, which is related to the displacement correlation as

$$\partial_s \partial_t \langle \mathbf{R}(\boldsymbol{\xi},t,s) \otimes \mathbf{R}(\boldsymbol{\xi}',t,s) \rangle = -\langle \mathbf{u}(\boldsymbol{\xi},t) \otimes \mathbf{u}(\boldsymbol{\xi}',s) \rangle - \langle \mathbf{u}(\boldsymbol{\xi},s) \otimes \mathbf{u}(\boldsymbol{\xi}',t) \rangle. \quad (6.1)$$

By taking the trace of Eq. (6.1) and considering the limit of $\boldsymbol{\xi}' - \boldsymbol{\xi} \to \mathbf{0}$, we obtain

$$\langle \mathbf{u}(t) \cdot \mathbf{u}(s) \rangle = -\tfrac{1}{2} \partial_s \partial_t [X_\parallel(\xi,t,s) + X_\perp(\xi,t,s)]|_{\xi=0} \tag{6.2}$$

in the 2D case, and substitution of Eq. (4.37) yields

$$\langle \mathbf{u}(t) \cdot \mathbf{u}(0) \rangle = -\frac{S}{4\pi\rho_0} t^{-2} < 0. \tag{6.3}$$

Thus the velocity autocorrelation is shown to have a negative tail, with the exponent -2 in the present case.

More generally, in the n_d-dimensional case, the expression on right-hand side of the relation

$$\langle \mathbf{u}(t) \cdot \mathbf{u}(s) \rangle = -\tfrac{1}{2} \lim_{\boldsymbol{\xi} \to \mathbf{0}} \partial_s \partial_t \langle \mathbf{R}(\boldsymbol{\xi},t,s) \cdot \mathbf{R}(\mathbf{0},t,s) \rangle \tag{6.4}$$

can be evaluated by means of the n_d-dimensional AP formula [31],

$$\begin{aligned} &\langle R_\alpha(\boldsymbol{\xi},t,s) R_\beta(\mathbf{0},t,s) \rangle \\ &\quad \propto \int \left[\frac{C_{\alpha\beta}(\mathbf{k},s,s) + C_{\alpha\beta}(\mathbf{k},t,t)}{2} - C_{\alpha\beta}(\mathbf{k},t,s) \right] \\ &\qquad \times \frac{e^{-i\mathbf{k}\cdot\boldsymbol{\xi}}}{k_\alpha k_\beta} d^{n_\mathrm{d}}\mathbf{k}, \end{aligned} \tag{6.5}$$

where $\alpha,\beta \in \{1,2,\ldots,n_\mathrm{d}\}$ and

$$C_{\alpha\beta}(\mathbf{k},t,s) = \frac{\rho_0^2}{N} \langle \check{\Psi}_\alpha(\mathbf{k},t) \check{\Psi}_\beta(-\mathbf{k},s) \rangle$$

denotes the correlation of the deformation gradient tensor defined in analogy with Eqs. (4.25)–(4.27). The correlation $C_{\alpha\beta}$ in the integrand of Eq. (6.5) will comprise exponential terms, analogous to Eqs. (4.16) and (4.33a) and making a negative contribution to the velocity autocorrelation, as well as a linear term such as Eq. (4.33b), whose contribution vanishes. Therefore, in total, the velocity autocorrelation must be negative. The exponent is evaluated as follows: Differentiating $C_{\alpha\alpha}$ in Eq. (6.5) with s and t, under the assumption that the exponential term in it has essentially the same k dependence as Eqs. (4.16) and (4.33a), we find

$$\begin{aligned} -\langle \mathbf{u}(t) \cdot \mathbf{u}(s) \rangle &= \frac{1}{2} \sum_\alpha \partial_t \partial_s \langle R_\alpha(\mathbf{0},t,s) R_\alpha(\mathbf{0},t,s) \rangle \\ &\propto \int e^{-D_*^\mathrm{c} k^2 (t-s)} k^2 \, d^{n_\mathrm{d}}\mathbf{k} \\ &\propto (t-s)^{-(n_\mathrm{d}+2)/2}. \end{aligned} \tag{6.6}$$

Setting $n_\mathrm{d} = 2$ in Eq. (6.6) reproduces the exponent -2 in Eq. (6.3). It is also consistent with the exponent $-5/2$ of the negative longtime tail in the 3D colloidal systems [48] and also with the 1D results [63,75] in which the exponent is $-3/2$. A result analogous to Eq. (6.6) was also reported by Hagen *et al.* [76] for a fluid confined in the quasi-n_d-dimensional space.

The temporal behavior of the velocity autocorrelation in Eqs. (6.3) and (6.6) clarifies that, in spite of the apparent resemblance of Fig. 1 to the back-flow structure observed in molecular dynamics by Alder and Wainwright [9], the two types of vortical cooperative motions originate from totally different mechanisms. The long-time tail of the velocity autocorrelation in Newtonian–Hamiltonian molecular dynamics is basically *positive*, resulting from conservation of vorticity (the rotational part of the momentum field). Contrastively, the velocity autocorrelation in colloidal systems is seen to have a *negative* tail. The negative value of $\langle \mathbf{u}(t) \cdot \mathbf{u}(0) \rangle$ is a manifestation of the cage effect: the particles are always pushed back by its neighbors. In this sense, the cage effect is successfully captured by the analytically calculated displacement correlations in Eq. (4.37), which directly lead to Eq. (6.3) describing the negative tail behavior.

Now, recalling our remark in the Introduction that the case of Newtonian molecular dynamics for dense liquids deserves special consideration, we note that the longtime tail in such systems can be rather complicated, as was reported by Williams *et al.* [77]. They studied Newtonian molecular dynamics of 3D hardcore fluids with various densities. For the lowest density, the velocity autocorrelation remains positive for all t, and the Alder-Wainwright longtime tail is clearly observed. For liquids with somewhat higher densities, the velocity autocorrelation is seen to be transiently negative but becomes positive again. For even higher densities in the "supercooled" regime, the positive long-time tail vanishes and the negative tail dominates. These findings of Williams *et al.* [77] could be interpreted, in light of Eq. (6.6), as follows: For Newtonian molecular dynamics with moderate densities, asymptotically $\langle \mathbf{u}(t) \cdot \mathbf{u}(0) \rangle$ will be expressible as a superposition of the Alder-Wainwright tail, $+At^{-n_\mathrm{d}/2}$, and the negative long-time tail due to the cage effect, $-Bt^{-(n_\mathrm{d}+2)/2}$, so that

$$\langle \mathbf{u}(t) \cdot \mathbf{u}(0) \rangle \sim +At^{-n_\mathrm{d}/2} - Bt^{-(n_\mathrm{d}+2)/2} \tag{6.7}$$

for such systems. The term with $+A$ is due to the conservation of vorticity, while that with $-B$ originates from the mass conservation. Since $t^{-n_\mathrm{d}/2}$ decays more slowly, the first term is expected to survive. As the density is increased, the coefficient A decreases and B increases, and finally A disappears (if we accept the conclusion of Williams *et al.* [77] that the Alder-Wainwright tail was not observed any more). This interpretation also seems to be consistent with the kinetic theory of monoatomic liquids by Sjögren and Sjölander [78], stating that the memory function due to the the density modes and that due to the vorticity modes contribute to the diffusion separately, with the former dominating at higher densities and the latter at lower.

Let us return to the displacement correlation in Eq. (4.37). It suggests that the MSD has a logarithmic correction term to the normal diffusion [31]. If we adopt the estimation

$$\langle [\mathbf{R}(t)]^2 \rangle \sim X_\parallel(\xi_\mathrm{cut},t) \tag{6.8}$$

with the "cutoff length" $\ell_0 \xi_\mathrm{cut}$, Eq. (4.37a) yields

$$\langle \mathbf{R}^2 \rangle \sim D_\alpha t + \frac{O(1)}{\rho_0} \ln \frac{Dt}{\sigma^2} \tag{6.9}$$

with $D_\alpha \sim D$ if $\xi_\mathrm{cut} \sim O(1)$.

The logarithmic term is characteristic of 2D caged particles and 2D elastic bodies. The dynamics of caged particles, for time scales shorter than τ_α, can be modeled by elastic network [6,79]; according to this modeling and on the assumption that continuum description is valid, the calculation of the MSD

reduces to the Edwards-Wilkinson integral [80,81], which leads to the logarithmic behavior. Recently another model that relates the caged diffusion to the Edwards-Wilkinson equation was studied by Centres and Bustingorry [82]. Their model consists of diffusing particles on a 2D lattice, with a constraint reminiscent of the eight-queens problem [83–85]. Since the cages never break in this model, the normal diffusion disappears. Centres and Bustingorry [82] showed that the computed MSD, in the case corresponding to the 2D version of the unbiased single-file diffusion, is consistent with the prediction of the 2D Edwards-Wilkinson equation. This behavior, which corresponds to Eq. (6.9) with $D_\alpha = 0$, is in contrast to the more usual 2D lattice dynamics of particles interacting through the excluded volume effect alone [86,87], in which the MSD takes the same form as in Eq. (6.9) with finite D_α; see Eq. (11) in Ref. [87]. Besides, in the case of colloidal liquids without lattice, such as the ones modeled by Eqs. (2.1)–(2.3) with $n_\mathrm{d} \geqslant 2$ and $V_\mathrm{max} \to +\infty$, Osada [88] has proven that D_α never vanishes for any finite temperature and pressure [3,88]. In the sense that nonzero D_α is incorporated together with the cage effect, the present analysis seems to be a step in the right direction as a theory of colloidal liquids.

B. Toward a mode-coupling theory of elasticity

Being a kind of four-point space-time correlation, the displacement correlation, $\langle \mathbf{R} \otimes \mathbf{R} \rangle$, delivers useful information about dynamics of dense liquids. The keystone in our analytical calculation of $\langle \mathbf{R} \otimes \mathbf{R} \rangle$ is the Alexander-Pincus formula: it relates the displacement correlation, a *four-point* statistical quantity, to the *two-body* correlation of the Lagrangian deformation gradient tensor. We have observed that, by way of the 2D Alexander-Pincus formula (4.34), the linear analysis of the Dean-Kawasaki equation already gives the longitudinal and transverse displacement correlations in Eq. (4.37), which captures both the nonzero D_α and the (precursory) caged dynamics.

Nevertheless, it is still problematic that the linear theory cannot be accurate enough. In particular, quantitative prediction of $D_\alpha = \lim_{t\to\infty} \langle \mathbf{R}^2 \rangle / (2n_\mathrm{d} t)$ is beyond its scope. The most serious limitation is found in the short-range behavior of $X_\perp$: according to Eq. (4.37b), the value of $X_\perp(\xi,t)$ remains negative for $\xi \to +0$, while it should be positive for sufficiently small ξ, as is suggested by the numerical results. Pictorially speaking, the distance between the centers of the vortices in Fig. 1 must be finite, but the linear theory predicts the distance to be zero, as is shown in Fig. 7(a).

As a remedy for this discrepancy, we take notice of Eq. (4.36) describing the contribution of C_r to the displacement correlation, and consider modification to it based on a nonlinear theory to go beyond Eq. (4.28). In the case of hard-core particles, the quadratic nonlinear terms can be calculated concretely, which leads to a set of nonlinear equations for ψ_d and ψ_r, in the following form:

$$(\partial_t + D_*^\mathrm{c}\mathbf{k}^2)\psi_\mathrm{d}(\mathbf{k},t) = \sum_{\mathbf{p}+\mathbf{q}+\mathbf{k}=\mathbf{0}} [\psi_\mathrm{d}^*(\mathbf{p},t) \quad \psi_\mathrm{r}^*(\mathbf{p},t)] \begin{bmatrix} \mathcal{V}_{\mathrm{d},\mathbf{k}}^{\mathrm{dd}}(\mathbf{p},\mathbf{q}) & \mathcal{V}_{\mathrm{d},\mathbf{k}}^{\mathrm{dr}}(\mathbf{p},\mathbf{q}) \\ \mathcal{V}_{\mathrm{d},\mathbf{k}}^{\mathrm{rd}}(\mathbf{p},\mathbf{q}) & \mathcal{V}_{\mathrm{d},\mathbf{k}}^{\mathrm{rr}}(\mathbf{p},\mathbf{q}) \end{bmatrix} \begin{bmatrix} \psi_\mathrm{d}^*(\mathbf{q},t) \\ \psi_\mathrm{r}^*(\mathbf{q},t) \end{bmatrix} + O(\psi^3) + \check{f}_\mathrm{d}(\mathbf{k},t), \tag{6.10a}$$

$$\partial_t \psi_\mathrm{r}(\mathbf{k},t) = \sum_{\mathbf{p}+\mathbf{q}+\mathbf{k}=\mathbf{0}} [\psi_\mathrm{d}^*(\mathbf{p},t) \quad \psi_\mathrm{r}^*(\mathbf{p},t)] \begin{bmatrix} \mathcal{V}_{\mathrm{r},\mathbf{k}}^{\mathrm{dd}}(\mathbf{p},\mathbf{q}) & \mathcal{V}_{\mathrm{r},\mathbf{k}}^{\mathrm{dr}}(\mathbf{p},\mathbf{q}) \\ \mathcal{V}_{\mathrm{r},\mathbf{k}}^{\mathrm{rd}}(\mathbf{p},\mathbf{q}) & 0 \end{bmatrix} \begin{bmatrix} \psi_\mathrm{d}^*(\mathbf{q},t) \\ \psi_\mathrm{r}^*(\mathbf{q},t) \end{bmatrix} + O(\psi^3) + \check{f}_\mathrm{r}(\mathbf{k},t), \tag{6.10b}$$

where $\check{f}_\mathrm{d}$ and $\check{f}_\mathrm{r}$ are random forces given by some appropriate linear combinations of $\check{f}_1$ and $\check{f}_2$ in Eq. (4.29). On the basis of a preliminary analysis of Eq. (6.10) [89], we may replace Eq. (4.36) with an equation analogous to Eq. (4.35),

$$\frac{C_\mathrm{r}(\mathbf{k},s,s) + C_\mathrm{r}(\mathbf{k},t,t)}{2} - C_\mathrm{r}(\mathbf{k},t,s) = \frac{1}{\mu_\mathrm{r} L^4}[1 - e^{-\mu_\mathrm{r} D_* \mathbf{k}^2 (t-s)}], \tag{6.11}$$

introducing a parameter μ_r. For $\mu_\mathrm{r} \to 0$, Eq. (6.11) reduces to Eq. (4.36). Positive values of μ_r change the behavior for large values of $D_*^\mathrm{c}\mathbf{k}^2(t-s)$, as Eq. (4.36) diverges linearly while Eq. (6.11) converges to $1/(\mu_\mathrm{r} L^4)$. The physical meaning of μ_r is suggested by noticing that Eq. (6.11) has the same structure as Eq. (4.35), with μ_r corresponding to S and D/μ_r to $D_*^\mathrm{c} = D_*/S$; since S is related to the compressibility, introducing μ_r in Eq. (6.11) means introducing the shear modulus. The inverse proportionality of the saturation value of C_r to μ_r seems to be consistent with this interpretation, as is seen from the recent studies by Klix *et al.* [26] and Flenner and Szamel [27]. More concretely, Eq. (6.11) can be rewritten in terms of $S_4^\perp(\mathbf{q},t)$ in Eq. (4.44), via Eq. (4.43), as

$$S_4^\perp(\mathbf{q},t-s) \propto \frac{1 - e^{-\mu_\mathrm{r} D q^2 (t-s)}}{\mu_\mathrm{r} q^2}; \tag{6.12}$$

assuming Eq. (6.11) therefore implies that, for $\ell_0^2 \ll q^{-2} \ll \mu_\mathrm{r} D(t-s)$, asymptotically $S_4^\perp(\mathbf{q},t-s)$ should behave in inverse proportion to $\mu_\mathrm{r} q^2$. Indeed, this behavior of $S_4^\perp(\mathbf{q},t-s)$ was recently demonstrated by Flenner and Szamel [27], for both glassy solids and liquids. In the latter case (dense liquids), however, it should be noted that the q^{-2} behavior was observed only transiently, and therefore the validity of Eq. (6.11) should be limited to some long but finite range of time.

Now let us study how the nonzero μ_r modifies the analytical expression of the displacement correlation. By substituting Eq. (6.11) into the Alexander-Pincus formula (4.34), together

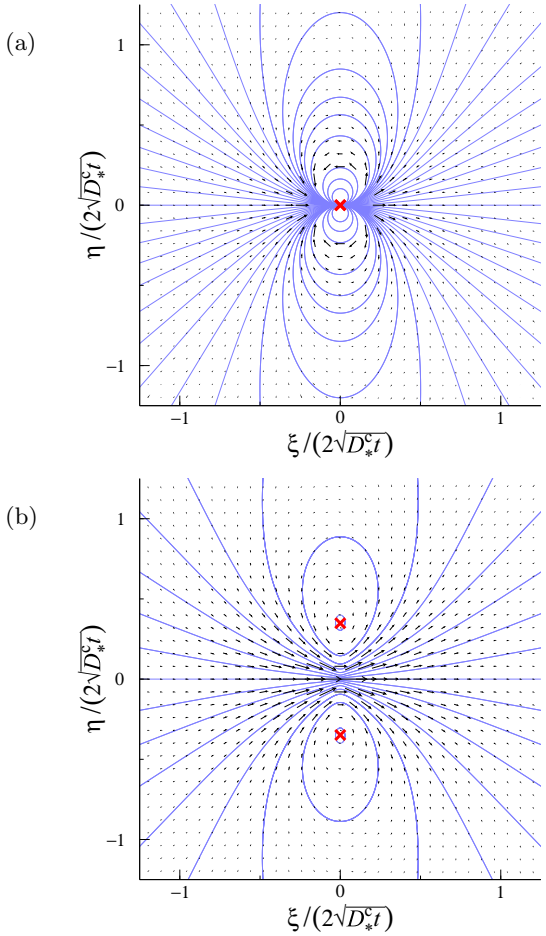

FIG. 7. Plot of the analytically calculated 2D displacement correlation. The value of $\mathbf{X}\cdot\mathbf{e}_1$ is plotted as a vector field on the $\boldsymbol{\xi}$ plane (normalized with $2\sqrt{D_*^c t}$), together with the "streamlines"; the crosses indicate the centers of the vortices. (a) The result of the linear theory in Eq. (4.37). (b) A modified plot based on Eq. (6.13), with $\mu_r = 0.25 > 0$.

with Eq. (4.35), Eq. (4.37) is modified as

$$X_\parallel(\xi,t) = \frac{S}{4\pi\rho_0}\left[E_1(\theta^2) + E_1(\theta^2/\mu_r) + \frac{e^{-\theta^2} - e^{-\theta^2/\mu_r}}{\theta^2}\right], \tag{6.13a}$$

$$X_\perp(\xi,t) = \frac{S}{4\pi\rho_0}\left[E_1(\theta^2) + E_1(\theta^2/\mu_r) - \frac{e^{-\theta^2} - e^{-\theta^2/\mu_r}}{\theta^2}\right]. \tag{6.13b}$$

Equation (6.13b) has the desirable property that $X_\perp$ is positive for small θ, so that the two vortices are now separated by a finite distance, as is shown in Fig. 7(b). In addition, $X_\parallel$ in Eq. (6.13a) also improves upon Eq. (4.37a), as is indicated by the broken line in Fig. 6, where $\mu_r = 0.13$ gives the best agreement.

Although μ_r is treated here as a fitting parameter, it should be determined from a nonlinear theory for Ψ, namely the mode-coupling theory for ψ_d and ψ_r. A nonlinear theory is needed also because the asymptotic behavior of Eq. (6.13a)

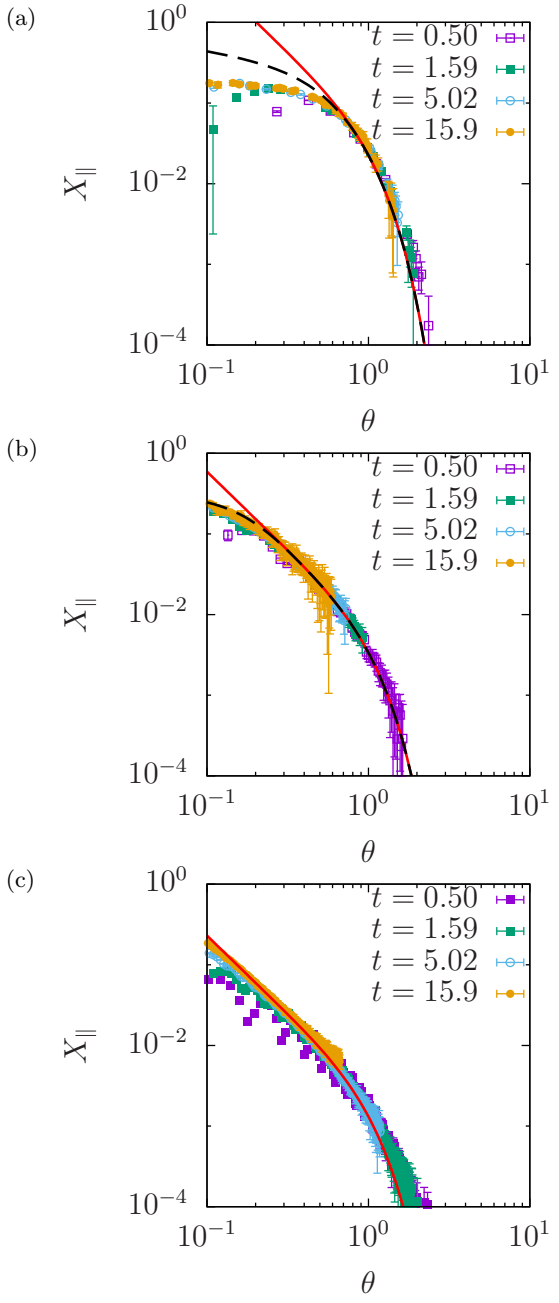

FIG. 8. Numerical values of $X_\parallel$ for different values of ϕ: (a) $\phi = 0.4$, (b) $\phi = 0.6$, and (c) $\phi = 0.7$, plotted basically in the same way as in Fig. 6. In the denser cases (b) and (c), greater values of V_{max} were used, in order to keep the computational condition close to that of hard spheres, which was confirmed by checking that the MSD does not depend on V_{max} any more. The values of V_{max} and $S = S(k \to +0)$, as well as that of the fitting parameter μ_r, are summarized as follows: (a) $V_{max} = 50\,k_BT$, $S = 0.246$, $\mu_r = 0.16$; (b) $V_{max} = 500\,k_BT$, $S = 0.055$, $\mu_r = 0.052$; and (c) $V_{max} = 5000\,k_BT$, $S = 0.025$, $\mu_r = 0$.

for $0 < \theta^2 \ll \mu_r < 1$ implies logarithmic MSD with $D_\alpha = 0$, which is the behavior of a soft elastic body but not that of a colloidal liquid. While Eq. (6.11) converges and Eq. (4.36) diverges rapidly for large $D_*^c\mathbf{k}^2(t-s)$, the truth is probably somewhere in between, as was suggested by the numerical behavior of $S_4^\perp(\mathbf{q},t)$ computed for glassy liquids [27]. We

expect that a nonlinear theory for Ψ will reveal the correct behavior of C_r, possibly predicting slow divergence of the expression on the left-hand side of Eqs. (4.36) and (6.11).

The idea of MCT for displacement correlation may sound infeasible, but in fact, the way is already paved to a certain extent. First, there is no need to develop a closure for four-body correlations, because *two-body* correlations, C_d and C_r, are sufficient as input into the Alexander-Pincus formula (4.34); this is the advantage of the Lagrangian description [30,31]. Second, the Lagrangian description has another advantage of changing the multiplicative noise in the Dean-Kawasaki equation into an additive one, which facilitates field-theoretical formalisms of MCT. Third, the coefficients in Eq. (6.10) can be concretely expressed, at least in the case of 2D hard-core particles. Encouraged by these conditions, and also motivated by the intuition that a theory about correlations of deformation gradient tensor will open a door to the rheology of glassy liquids, we have started a preliminary analysis of an MCT-like equations for C_d and C_r [89]. An effort in this direction is now in progress and will be reported elsewhere.

Finally, in order to see how the validity of the present theory depends on the area fraction, we computed $X_\parallel$ for three different values of ϕ, in addition to $\phi = 0.5$ reported in Sec. VI. The numerical results are summarized in Fig. 8, where $X_\parallel$ is plotted against the similarity variable θ. It seems to be valid in all the cases, or, at least, except for the case of $\phi = 0.7$ in which evidence may be insufficient, that $X_\parallel(\xi,t)$ for different t is expressible through the similarity variable θ, and reasonable agreement is found near $\theta \sim 1$. Although the discrepancy in the short-range behavior remains in all the cases, the remedy with μ_r seems to be effective for $\phi = 0.6$ [the broken line in Fig. 8(b)]. In the high-density case ($\phi = 0.7$), while the short-range discrepancy is small for $t = 15.9$, the correlation for $\theta > 1$ becomes somewhat greater than the prediction of the linear theory in Eq. (4.40a); the behavior seems to approach the exponential decay, $X_\parallel \propto e^{-\theta}$, in agreement with Doliwa and Heuer [5]. This enhancement of the displacement correlation for $\theta > 1$ in the high-density case is out of the scope of the linear theory, but the self-similarity still seems to hold, raising the hope that the analytical method in Sec. IV could be somehow extended to this case, possibly in the form of field-theoretical development of MCT-like equations and their approximate solution in terms of a similarity variable.

VII. CONCLUDING REMARKS

Starting from the Dean-Kawasaki equation (2.6) that gives a mesoscopic continuum description of colloidal liquids, we have developed an analytical calculation of the displacement correlation tensor $\langle \mathbf{R} \otimes \mathbf{R} \rangle$ and compared the analytical results with direct numerical simulation of interacting Brownian particles. The results of the linear analysis, given in Eq. (4.37), already include information about the basic space-time structure of the cooperative motion, capturing its self-similar character, the vortical flow pattern, and the negative longtime tail.

The short-range behavior, however, needs to be improved on the basis of a nonlinear analysis. While the full analysis of Eq. (6.10) clearly belongs to our future work, for the present we have shown a numerical evidence that the analytical results are remarkably improved by introducing μ_r via Eq. (6.11). This is equivalent to introducing some finite value of shear modulus. As a result, Eq. (4.37) is replaced with Eq. (6.13), and the centers of the two vortices, shown in Fig. 7(b), are now separated by a finite distance, in agreement with the numerical plot in Fig. 1.

The present approach has several advantages. Among various four-point space-time correlations, the displacement correlation $\langle \mathbf{R} \otimes \mathbf{R} \rangle$ seems to be the most intuitive one. The calculated results allow pictorial presentation as in Figs. 1 and 7, which must be helpful in intuitive understanding of cooperative motions. In previous studies of colloidal systems, this comprehensibility of the displacement correlation was available only at a great cost, as it needed to be calculated from particle-based data. Now we have discovered a route connecting the displacement correlation tensor and the Dean-Kawasaki equation, which, in principle, makes it possible to calculate $\langle \mathbf{R} \otimes \mathbf{R} \rangle$ without resorting to direct numerical simulation of particles.

From the viewpoint of the future work, in which the displacement correlation will be calculated on the basis of the nonlinear equation (6.10), the main significance of the present article would be its methodology. It has laid foundation for tensorial MCT to be developed in this future work. The adoption of the Lagrangian description has made it possible to calculate $\langle \mathbf{R} \otimes \mathbf{R} \rangle$, which itself is a four-point correlation, from two-body correlations such as C_d and C_r. The Lagrangian description has also expelled the ρ dependence from the random force of the Dean-Kawasaki equation, thus removing an obstacle for the field-theoretical development of MCT.

We must admit, on one hand, that still some issues are to be settled before the plan of tensorial MCT is realized. Due to the change of variables, the rewritten version of the Dean-Kawasaki equation has an infinite number of nonlinear terms. It is not clear under what condition the higher-order terms can be ignored. Probably some of the terms must be retained so as to respect certain kinds of symmetry, such as those with regard to time-translation and relabeling. It is also necessary to develop equations that determine the "initial values" of $C_d(\mathbf{k},t,s)$ and $C_r(\mathbf{k},t,s)$ for $t = s$, because it is not evident how the initial value of C_d is related to S in general, and also because C_r seems to involve a kind of apparent aging.

On the other hand, if these issues are settled successfully or turn out to be harmless, the tensorial MCT will be quite fruitful. It will shed light of analytical treatments on the cooperative dynamics in glassy liquids. By determining the behavior of C_r and thus giving the value of μ_r, it provides information of the shear modulus, and its extension with shear flow will give a direct access to the rheology of colloidal suspensions. Besides, since Eq. (6.10) has nonlinear terms that couple ψ_d and ψ_r mutually, the vortical motion involving C_r may influence the dynamics of C_d that govern the cage collapse. The tensorial MCT may clarify how this coupling modifies the predictions of the standard MCT based on the dilatational modes alone. We hope that the present work will contribute to this quite intriguing nonlinear theory, in which both the dilatational and the rotational modes are coupled with each other under the overdamped Dean-Kawasaki dynamics.

ACKNOWLEDGMENTS

We express our cordial gratitude to Hajime Yoshino, Atsushi Ikeda, Takahiro Hatano, Kunimasa Miyazaki, Ferenc Kun, Grzegorz Szamel, Tadashi Muranaka, Hisao Hayakawa, Ken Sekimoto, Akio Nakahara, and So Kitsunezaki for fruitful discussions, including thought-provoking questions and insightful comments. We also thank Alexander Mikhailov, not only for such discussions, but also for pointing out some old instances of the diffusion equation with multiplicative noise, including Ref. [42], whose first edition dates back to 1983. Anonymous referees are acknowledged for helpful comments and for drawing our attention to Ref. [27]. This work was supported by Grants-in-Aid for Scientific Research (Kakenhi) (C) No. 24540404 and No. 15K05213, JSPS (Japan).

[1] Y. Hiwatari and T. Muranaka, J. Non-Cryst. Solids **235–237**, 19 (1998).
[2] R. Yamamoto and A. Onuki, Phys. Rev. E **58**, 3515 (1998).
[3] L. Berthier and G. Biroli, Rev. Mod. Phys. **83**, 587 (2011).
[4] *Dynamical Heterogeneities in Glasses, Colloids, and Granular Media*, edited by L. Berthier, G. Biroli, J.-P. Bouchaud, L. Cipelletti, and W. van Saarloos (Oxford University Press, Oxford, 2011).
[5] B. Doliwa and A. Heuer, Phys. Rev. E **61**, 6898 (2000).
[6] C. Brito and M. Wyart, J. Chem. Phys. **131**, 024504 (2009).
[7] S. Sota and M. Itoh, J. Korean Phys. Soc. **54**, 386 (2009).
[8] A. Ghosh, V. K. Chikkadi, P. Schall, J. Kurchan, and D. Bonn, Phys. Rev. Lett. **104**, 248305 (2010).
[9] B. J. Alder and T. E. Wainwright, Phys. Rev. A **1**, 18 (1970).
[10] T. P. C. van Noije and M. H. Ernst, Phys. Rev. E **61**, 1765 (2000).
[11] T. Vicsek and A. Zafeiris, Phys. Rep. **517**, 71 (2012).
[12] U. Frisch, *Turbulence: The Legacy of A.N. Kolmogorov* (Cambridge University Press, Cambridge, 1995).
[13] G. K. Batchelor, *The Theory of Homogeneous Turbulence* (Cambridge University Press, Cambridge, 1953).
[14] J. O. Hinze, *Turbulence,* 2nd ed. (McGraw-Hill, New York, 1975).
[15] L. D. Landau and E. M. Lifshitz, *Fluid Mechanics*, Vol. 6 of Theoretical Physics (Butterworth-Heinemann, Oxford, 1987).
[16] P. Saffman and D. Pullin, Phys. Fluids **8**, 3072 (1996).
[17] D. Pullin and P. Saffman, Annu. Rev. Fluid Mech. **30**, 31 (1998).
[18] C. Dasgupta, A. V. Indrani, S. Ramaswamy, and M. K. Phani, Europhys. Lett. **15**, 307 (1991).
[19] S. C. Glotzer, V. N. Novikov, and T. B. Schrøder, J. Chem. Phys. **112**, 509 (2000).
[20] G. Szamel and H. Löwen, Phys. Rev. A **44**, 8215 (1991).
[21] T. Gleim, W. Kob, and K. Binder, Phys. Rev. Lett. **81**, 4404 (1998).
[22] L. Berthier, G. Biroli, J.-P. Bouchaud, W. Kob, K. Miyazaki, and D. R. Reichman, J. Chem. Phys. **126**, 184503 (2007).
[23] G. Szamel, J. Chem. Phys. **127**, 084515 (2007).
[24] T. Muranaka and Y. Hiwatari, Phys. Rev. E **51**, R2735 (1995).
[25] C. Donati, S. C. Glotzer, and P. H. Poole, Phys. Rev. Lett. **82**, 5064 (1999).
[26] C. L. Klix, F. Ebert, F. Weysser, M. Fuchs, G. Maret, and P. Keim, Phys. Rev. Lett. **109**, 178301 (2012).
[27] E. Flenner and G. Szamel, Phys. Rev. Lett. **114**, 025501 (2015).
[28] A. Ikeda and L. Berthier, Phys. Rev. E **92**, 012309 (2015).
[29] S. Bernini and D. Leporini, J. Chem. Phys. **144**, 144505 (2016).
[30] T. Ooshida, S. Goto, T. Matsumoto, A. Nakahara, and M. Otsuki, Phys. Rev. E **88**, 062108 (2013).
[31] T. Ooshida, S. Goto, T. Matsumoto, and M. Otsuki, Biophys. Rev. Lett. **11**, 9 (2016).
[32] L. Berthier and T. A. Witten, Europhys. Lett. **86**, 10001 (2009).
[33] For the interaction potential V_{jk} we could have used any soft-core potential that has a proper hard-core limit. Here we adopted the repulsive harmonic sphere in Eq. (2.3), simply because its hard-core limit has been investigated systematically [32].
[34] P. M. Chaikin and T. C. Lubensky, *Principles of Condensed Matter Physics* (Cambridge University Press, Cambridge, 1995).
[35] S. P. Das and A. Yoshimori, Phys. Rev. E **88**, 043008 (2013).
[36] N. Bidhoodi and S. P. Das, Phys. Rev. E **92**, 012325 (2015).
[37] D. S. Dean, J. Phys. A: Math. Gen. **29**, L613 (1996).
[38] K. Kawasaki, Physica A **208**, 35 (1994).
[39] K. Kawasaki, J. Stat. Phys. **93**, 527 (1998).
[40] S. P. Das, *Statistical Physics of Liquids at Freezing and Beyond* (Cambridge University Press, New York, 2011).
[41] B. Kim, K. Kawasaki, H. Jacquin, and F. van Wijland, Phys. Rev. E **89**, 012150 (2014).
[42] C. W. Gardiner, *Stochastic Methods: A Handbook for the Natural and Social Sciences,* 4th ed. (Springer-Verlag, Berlin, 2009).
[43] A. Mikhailov and A. Loskutov, *Foundations of Synergetics. II. Chaos and Noise,* 2nd ed. (Springer, Berlin, 1996).
[44] N. G. van Kampen, *Stochastic Processes in Physics and Chemistry,* 3rd ed. (Elsevier, Amsterdam, 2007).
[45] K. Kawasaki, in *Synergetics: Cooperative Phenomena in Multi-Component Systems (Proceedings of the Symposium on Synergetics, 1972, Elmau)*, edited by H. Haken (B. G. Teubner, Stuttgart, 1973), pp. 35–44.
[46] K. Kawasaki and T. Koga, Physica A **201**, 115 (1993).
[47] M. Hildebrand and A. S. Mikhailov, J. Phys. Chem. **100**, 19089 (1996).
[48] J. K. G. Dhont, *An Introduction to Dynamics of Colloids* (Elsevier, Amsterdam, 1996).
[49] S. P. Das, Rev. Mod. Phys. **76**, 785 (2004).
[50] K. Miyazaki and D. R. Reichman, J. Phys. A: Math. Gen. **38**, L343 (2005).
[51] A. Andreanov, G. Biroli, and A. Lefèvre, J. Stat. Mech. (2006) P07008.
[52] B. Kim and K. Kawasaki, J. Phys. A: Math. Theor. **40**, F33 (2007).
[53] B. Kim and K. Kawasaki, J. Stat. Mech. (2008) P02004.
[54] See Eq. (5.6) in Ref. [30].
[55] T. Ooshida, S. Goto, T. Matsumoto, and M. Otsuki, Mod. Phys. Lett. B **29**, 1550221 (2015).
[56] If $V_{\max}$ is finite and allows overtaking, it is necessary to specify the timing of renumbering to make $\langle R_i R_j \rangle$ meaningful [55].
[57] T. Ooshida, S. Goto, T. Matsumoto, A. Nakahara, and M. Otsuki, J. Phys. Soc. Jpn. **80**, 074007 (2011).

[58] L. Lizana, T. Ambjörnsson, A. Taloni, E. Barkai, and M. A. Lomholt, Phys. Rev. E **81**, 051118 (2010).
[59] P. M. Centres and S. Bustingorry, Phys. Rev. E **81**, 061101 (2010).
[60] M. Doi and S. F. Edwards, *The Theory of Polymer Dynamics* (Oxford University Press, Oxford, 1986).
[61] S. N. Majumdar and M. Barma, Physica A **177**, 366 (1991).
[62] H. Spohn, J. Stat. Phys. **154**, 1191 (2014).
[63] H. van Beijeren, K. W. Kehr, and R. Kutner, Phys. Rev. B **28**, 5711 (1983).
[64] B. Bakhti, M. Karbach, P. Maass, M. Mokim, and G. Müller, Phys. Rev. E **89**, 012137 (2014).
[65] S. Alexander and P. Pincus, Phys. Rev. B **18**, 2011 (1978).
[66] Once the relation between x and ξ is established, the problem of rewriting (fluctuating) hydrodynamic equations such as Eqs. (2.5) and (2.6) into the form of Eq. (4.13) is simply an exercise in change of variables. See the procedure following Eq. (3.7) in Ref. [57], as well as Appendix 5 in Ref. [62].
[67] In the calculation leading to Eq. (4.18), the value of $C(k,0)$ is needed as the initial value of $C(k,t)$. We can assume $C(k,0) = S(0)/L^2$, which seems to be valid within the long-wave approximation.
[68] H. Shiba, T. Kawasaki, and A. Onuki, Phys. Rev. E **86**, 041504 (2012).
[69] T. Kawasaki and A. Onuki, Phys. Rev. E **87**, 012312 (2013).
[70] S. Sabhapandit and A. Dhar, J. Stat. Mech. (2015) P07024.
[71] J. E. Marsden and T. J. Hughes, *Mathematical Foundations of Elasticity* (Dover Publications, New York, 1994).
[72] R. B. Bird, R. C. Armstrong, and O. Hassager, *Dynamics of Polymeric Liquids*, 2nd ed. (Wiley, New York, 1987), Vol. 1.
[73] T. Ooshida, Phys. Rev. E **77**, 061501 (2008).
[74] G. Arfken, H.-J. Weber, and F. Harris, *Mathematical Methods for Physicists: A Comprehensive Guide,* 7th ed. (Elsevier Academic Press, Waltham, 2013).
[75] A. Taloni and M. A. Lomholt, Phys. Rev. E **78**, 051116 (2008).
[76] M. H. J. Hagen, I. Pagonabarraga, C. P. Lowe, and D. Frenkel, Phys. Rev. Lett. **78**, 3785 (1997).
[77] S. R. Williams, G. Bryant, I. K. Snook, and W. van Megen, Phys. Rev. Lett. **96**, 087801 (2006).
[78] L. Sjögren and A. Sjölander, J. Phys. C **12**, 4369 (1979).
[79] C. Brito and M. Wyart, Europhys. Lett. **76**, 149 (2006).
[80] S. F. Edwards and D. R. Wilkinson, Proc. R. Soc. London A **381**, 17 (1982).
[81] C. Toninelli, M. Wyart, L. Berthier, G. Biroli, and J.-P. Bouchaud, Phys. Rev. E **71**, 041505 (2005).
[82] P. M. Centres and S. Bustingorry, Phys. Rev. E **93**, 012134 (2016).
[83] J. Bell and B. Stevens, Discrete Math. **309**, 1 (2009).
[84] D. S. Dean and G. Parisi, J. Phys. A: Math. Gen. **31**, 3949 (1998).
[85] K. Hukushima, Comput. Phys. Commun. **147**, 77 (2002).
[86] K. Nakazato and K. Kitahara, Prog. Theor. Phys. **64**, 2261 (1980).
[87] H. van Beijeren and R. Kutner, Phys. Rev. Lett. **55**, 238 (1985).
[88] H. Osada, Probab. Theory Relat. Fields **112**, 53 (1998).
[89] T. Ooshida, M. Otsuki, S. Goto, and T. Matsumoto, in *Meeting Abstracts of the Physical Society of Japan (2015 Annual Meeting)* (Physical Society of Japan, Tokyo, 2015), p. 3095.